SIAM J. NUMER. ANAL.
Vol. 61, No. 3, pp. 1449–1481

TWOFOLD SADDLE-POINT FORMULATION OF BIOT POROELASTICITY WITH STRESS-DEPENDENT DIFFUSION*

BRYAN GÓMEZ-VARGAS†, KENT-ANDRÉ MARDAL‡, RICARDO RUIZ-BAIER§, AND VEGARD VINJE¶

Abstract. We present a new stress/total-pressure formulation for poroelasticity that incorporates the coupling with steady nonlinear diffusion modified by stress. This nonlinear problem is written in mixed-primal form, which combines a perturbed twofold saddle-point system with an elliptic problem. We analyze the continuous formulation within the framework of abstract fixed-point theory and Fredholm alternative for compact operators. A mixed finite element method is proposed, and its stability and convergence are rigorously analyzed. We also provide a few representative numerical examples to illustrate the effectiveness of the proposed formulation. The resulting model can be used to study the steady case of waste removal in the brain, providing insight into the transport of solutes in poroelastic structures under the influence of stress.

Key words. stress-altered diffusion, poroelasticity, perturbed saddle-point, mixed finite elements

MSC codes. 65N60, 92C50

DOI. 10.1137/21M1449695

1. Introduction.

Poroelastic structures are found in many applications of industrial and scientific relevance. Examples include the interaction between soft permeable tissue and blood flow or the study of biofilm growth and distribution near fluids [49]. We are concerned with one particular application involving the transport of cerebrospinal fluid (CSF) and tracer within the brain parenchyma and how this can contribute to better explain the mechanisms that permit solutes from the brain interstitial space to move. These processes are key in eliminating waste from the brain and in maintaining a healthy function of the nervous system (see, for instance, the review [43]), which address important questions in the context of the overall glymphatic function [33].

*Received by the editors September 30, 2021; accepted for publication (in revised form) February 6, 2023; published electronically June 12, 2023.
https://doi.org/10.1137/21M1449695

Funding: The work of the first author was supported by the Vicerrectoría de Investigación project 540-C0-202, Sede de Occidente, Universidad de Costa Rica. The work of the second author was supported by the Research Council of Norway grants 300305 and 301013. The work of the third author was supported by the Monash Mathematics Research Fund grant S05802-3951284, by the Australian Research Council through the FUTURE FELLOWSHIP grant FT220100496 and DISCOVERY PROJECT grant DP22010316, and by the Ministry of Science and Higher Education of the Russian Federation within the framework of state support for the creation and development of World-Class Research Centers DIGITAL BIODESIGN AND PERSONALIZED HEALTHCARE grant 075-15-2022-304.

†Sección de Matemática, Sede de Occidente, Universidad de Costa Rica, San Ramón, Alajuela, Costa Rica (bryan.gomezvargas@ucr.ac.cr).

‡Department of Mathematics, Division of Mechanics, University of Oslo, Oslo, Norway; and Simula Research Laboratory, 1325 Lysaker, Norway (kent-and@math.uio.no).

§School of Mathematics, Monash University, 9 Rainforest Walk, Melbourne 3800 VIC, Australia; and World-Class Research Center "Digital biodesign and personalized healthcare," Sechenov First Moscow State Medical University, Moscow, Russia; and Universidad Adventista de Chile, Casilla 7-D, Chillán, Chile (ricardo.ruizbaier@monash.edu).

¶Department for Numerical Analysis and Scientific Computing, Simula Research Laboratory, Lysaker, Norway (vegard@simula.no).

Detailed maps of permeability and simulations using realistic hydrostatic pressure gradients and image-based reconstruction of intersitial space suggest that diffusive effects along vasculature dominate over bulk flow [31]. However it appears that (even heterogeneous) Fickian diffusion and convective effects only are not sufficient to explain the main features of the physiological propagation of solutes along the various elements of the brain structure [13, 52]. We thus reconsider how other changes related to the mechanical state, such as the generation and nonuniform localization of stresses in the brain, could impact the filtration properties at the spatio-temporal scales of interest for the application at hand. Pressure, strain, and stress changes can affect the tissue microstructure by rearranging the local distribution of compliant arrays, opening and closing pores, and generating preferential paths for the accumulation of large solvent molecules [58]. The combination of such effects can result in variations of averaged coefficients usually employed in classical models, such as diffusion (but also other parameters such as bulk moduli, relative permeability, and the Biot–Willis coefficient [41]). For this effect we propose a simplified phenomenological model for the steady interaction between poroelastic stress and diffusion of solutes (such as gadobutrol). The coupling of poromechanics and diffusion is a fundamental aspect not only for investigating the mechanical behavior of the brain function but also in the description and design of other complex systems such as tissue engineering scaffolds [12].

Linear models of poroelasticity seem to be sufficient to capture the most important strain patterns when coupled to, e.g., immune system equations modeling the blood-brain barrier in the brain (see the comparison in [36]). In the present model the linear poroelasticity equations are formulated using the stress as an unknown. This is of particular importance, as this field will be central to the coupling with the diffusion process. The recent literature contains various formulations for Biot equations using poroelastic stress, for instance, including weakly symmetric three-field formulations [5, 37], four-field schemes [55], adaptive mixed formulations [17], multipoint stress-flux mixed methods [2], and domain decomposition approaches [34]. In contrast, here we employ a double saddle-point formulation designed to solve for total poroelastic stress, displacement, rotation, total pressure (drawing inspiration from [38, 42] and generalizing these formulations to include poroelastic and active stress), and fluid pressure. The Biot equations are then coupled with a nonlinear diffusion equation for the CSF tracer, and the discretization proceeds with classical mixed-primal finite elements. Weak imposition of symmetry in the poroelastic stress is required to enforce the balance of angular momentum when using H(div)-conforming approximations of stresses [3, 4], but using this approach may also have benefits in terms of computational cost versus discretizations of poroelasticity in primal variables [37].

Mixed-primal and fully mixed methods for stress-modified diffusion problems have been investigated in [23, 24], and their analysis hinges on techniques using a separation of elastostatics and diffusion equations by means of a fixed-point scheme that requires additional assumptions on regularity. This is precisely the approach followed here. These models, as well as modification of transport properties in other soft tissues such as cardiac muscle [45], allow us to recover enhanced anisotropy and heterogeneity of stress-assisted diffusion. However, here the coupling with total poroelastic stress is used to *reduce* or hinder diffusion patterns which have the potential to produce a much better match with experimental studies that indicate a decrease of effective diffusion by at least an order of magnitude with respect to the base state observed during sleep. For the sake of simplicity and convenience in the analysis we restrict ourselves to the stationary case—except for the tests related to the application in brain

modeling. Even the steady case is a source of a number of challenges. One of the main difficulties of the present work lies in deriving a variational formulation involving total poroelastic stress and whose analysis does not need additional conditions on the Lamé parameters. The resulting form has the structure of a double saddle-point problem, where terms that explicitly involve λ_s appear. Exploiting the compactness of these terms and applying the Fredholm alternative together with a new extended version of the Babuška–Brezzi theory allow us to assert unique solvability robustly with respect to λ_s.

The content of this paper has been laid out as follows. Section 2 provides details of the model, describing the components of the balance equations and stating boundary conditions. Section 3 is devoted to the analysis of solvability of the weak form, using fixed-point arguments in conjunction with the Fredholm alternative and the Babuška–Brezzi theory. We address in section 4 the solvability and stability analysis of the discrete problem. A priori error estimates are derived in section 5, and in section 6 we collect computational results, consisting in verification of convergence and simulation of different cases on simple geometries. We close with some remarks and discussion on model extensions in section 7.

2. Governing equations. Let us consider a Lipschitz polyhedral domain $\Omega \subset \mathbb{R}^d$, $d = 2, 3$ occupied by the brain parenchyma, here modeled as a mixture consisting of an elastic structure and an interconnected porous space fully saturated by interstitial fluid. We will denote by $\boldsymbol{n}$ the outward unit normal vector on the boundary $\partial\Omega$. We also define the boundaries Γ and Σ where different types of boundary conditions will be applied. We assume that the parenchyma is isotropic, that the deformation process is stationary, and that its constitutive stress-strain relation is linear. As usual in the framework of linear poroelasticity, the solid-fluid mixture is described in terms of the solid displacement $\boldsymbol{u} : \Omega \to \mathbb{R}^d$ accounting for the movement of the material from its initial undeformed configuration and the pore fluid pressure $p : \Omega \to \mathbb{R}$ (which, through Darcy's law, also defines the specific discharge or filtration velocity). The Biot system states momentum and mass balances

$$\begin{aligned} -\mathbf{div}(\boldsymbol{\sigma}) &= \rho_s \boldsymbol{f} \quad \text{in } \Omega, \\ c_0 p + \alpha \mathrm{div}(\boldsymbol{u}) - \mathrm{div}\left(\frac{\kappa}{\mu_f}\nabla p - \rho_f \boldsymbol{g}\right) &= m \quad \text{in } \Omega, \end{aligned} \tag{2.1}$$

respectively, where $\boldsymbol{f} : \Omega \to \mathbb{R}^d$ is the vector field of body loads and $m : \Omega \to \mathbb{R}$ is a source/sink of fluid. We also consider the presence of a CSF tracer within the poroelastic parenchymal domain. We denote its concentration by $\omega : \Omega \to \mathbb{R}$ and its movement in the parenchyma is governed by

$$\phi\omega - \mathrm{div}(D(\boldsymbol{\sigma})\nabla\omega) = \phi\ell \quad \text{in } \Omega, \tag{2.2}$$

where $\boldsymbol{\sigma} = 2\mu_s\boldsymbol{\varepsilon}(\boldsymbol{u}) + (\lambda_s \mathrm{div}(\boldsymbol{u}) - \alpha p - \beta\omega)\mathbb{I}$ is the poroelastic Cauchy stress tensor with $\boldsymbol{\varepsilon}(\boldsymbol{u}) := \frac{1}{2}(\nabla\boldsymbol{u} + \nabla\boldsymbol{u}^{\mathsf{t}})$ denoting the infinitesimal strain tensor, the Lamé constants $\mu_s, \lambda_s > 0$ for homogeneous and isotropic materials, the Biot–Willis constant $0 < \alpha \leq 1$, the $d \times d$ identity matrix $\mathbb{I}$, and β a scaling of active stress that indicates a two-way coupling between diffusion and motion. The right-hand side $\ell : \Omega \to \mathbb{R}$ is a nonnegative drainage or source coefficient that encodes absorption from the lymph nodes and/or from capillaries [14], and ϕ is porosity. In (2.1) c_0 is the mass storativity coefficient, and κ is the permeability tensor (symmetric, uniformly positive definite, and bounded). The tensor function $D : \mathbb{R}^{d\times d} \to \mathbb{R}^{d\times d}$ is a stress-dependent diffusivity

accounting for an altered diffusion acting in the poroelastic domain. This term may assume the simple form

$$D(\boldsymbol{\sigma}) = [\eta_0 D_0 + \eta_1 \exp(-\eta_1 \mathrm{tr}\boldsymbol{\sigma})]\mathbb{I}, \tag{2.3}$$

with D_0 being the effective diffusion of typical solutes such as potassium ions and η_0, η_1 modulating the intensity of the stress-altered diffusion. Other constitutive equations (including power-law, polynomial, and anisotropic forms) can be found in, e.g., [23], whereas pressure-dependent diffusion models can be found in [30]. Alternative constitutive relations could be given by a dependence on the volumetric part of the effective poroelastic stress or on the porosity (which in the linear regime is the total amount of fluid) such as $D = D_0\mathbb{I} - \eta(c_0 p + \alpha \mathrm{div}\boldsymbol{u})\mathbb{I}$. We prescribe tracer concentration on $\partial\Omega$, whereas we fix displacement and normal specific discharge on the boundary Γ and zero normal total stress and prescribed fluid pressure on Σ.

Besides the main variables we also employ the total pressure (the volumetric contributions to the poroelastic Cauchy stress) $\tilde{p} := \alpha p - \lambda_s \operatorname{div} \boldsymbol{u}$, the poroelastic stress tensor $\boldsymbol{\sigma} = 2\mu_s \boldsymbol{\varepsilon}(\boldsymbol{u}) - \tilde{p}\mathbb{I} - \beta\omega\mathbb{I}$, the tensor $\boldsymbol{\gamma}$ (rotation Lagrange multiplier assisting the weakly imposition of the symmetry of $\boldsymbol{\sigma}$), and the strain $\boldsymbol{t} := \boldsymbol{\varepsilon}(\boldsymbol{u}) = \nabla\boldsymbol{u} - \boldsymbol{\gamma}$. Therefore the governing equations consist in finding $\boldsymbol{\sigma}$, $\boldsymbol{u}$, $\boldsymbol{\gamma}$, $\boldsymbol{t}$, $\tilde{p}$, p, and ω, satisfying

$$\boldsymbol{t} = \boldsymbol{\varepsilon}(\boldsymbol{u}) \quad \text{in } \Omega, \tag{2.4a}$$

$$\boldsymbol{\sigma} = 2\mu_s \boldsymbol{t} - \tilde{p}\mathbb{I} - \beta\omega\mathbb{I} \quad \text{in } \Omega, \tag{2.4b}$$

$$\boldsymbol{\gamma} = \nabla\boldsymbol{u} - \boldsymbol{t} \quad \text{in } \Omega, \tag{2.4c}$$

$$\boldsymbol{\sigma} = \boldsymbol{\sigma}^{\mathrm{t}} \quad \text{in } \Omega, \tag{2.4d}$$

$$-\mathbf{div}\,\boldsymbol{\sigma} = \rho_s \boldsymbol{f} \quad \text{in } \Omega, \tag{2.4e}$$

$$\left(c_0 + \frac{\alpha^2}{\lambda_s}\right) p - \frac{\alpha}{\lambda_s}\tilde{p} - \operatorname{div}\left(\frac{\kappa}{\mu_f}\nabla p - \rho_f \boldsymbol{g}\right) = m \quad \text{in } \Omega, \tag{2.4f}$$

$$\frac{1}{\lambda_s}\tilde{p} + \mathrm{tr}\boldsymbol{t} - \frac{\alpha}{\lambda_s} p = 0 \quad \text{in } \Omega, \tag{2.4g}$$

$$\phi\omega - \mathrm{div}(D(\boldsymbol{\sigma})\nabla\omega) = \phi\ell \quad \text{in } \Omega, \tag{2.4h}$$

$$\boldsymbol{u} = \boldsymbol{0}, \quad \frac{\kappa}{\mu_f}\nabla p \cdot \boldsymbol{n} = 0 \quad \text{on } \Gamma, \quad \boldsymbol{\sigma}\boldsymbol{n} = \boldsymbol{0}, \quad p = 0 \quad \text{on } \Sigma, \tag{2.4i}$$

$$\omega = 0 \quad \text{on } \partial\Omega. \tag{2.4j}$$

Equations (2.4d)–(2.4e) state, respectively, the conservation of angular and linear momentums, while (2.4b), (2.4a), (2.4c), and (2.4g) encode constitutive relations for stress, strain, rotations, and total pressure, respectively. Homogeneous boundary conditions (2.4i)–(2.4j) have been assumed only for the sake of conciseness, but they can be generalized to the nonhomogeneous case by using classical lifting arguments. An advantage of using this modified form of the system is that all equations are robust with respect to the Lamé parameters.

3. Continuous mixed-primal formulation and well-posedness analysis. Let us define the tensor functional spaces for stress and rotations and the scalar field for the pressure,

$$\mathbb{H}_\Sigma(\mathbf{div},\Omega) := \{\boldsymbol{\tau} \in \mathbb{H}(\mathbf{div},\Omega) : \boldsymbol{\tau}\boldsymbol{n} = \boldsymbol{0} \text{ on } \Sigma\}, \ \mathbb{L}^2_{\mathrm{skew}}(\Omega) := \{\boldsymbol{\eta} \in \mathbb{L}^2(\Omega) : \boldsymbol{\eta} + \boldsymbol{\eta}^{\mathrm{t}} = \boldsymbol{0}\},$$

$$\mathrm{H}^1_\Sigma(\Omega) := \{q \in \mathrm{H}^1(\Omega) : q = \boldsymbol{0} \text{ on } \Sigma\}.$$

A weak formulation for the linear poroelasticity problem (2.4a)–(2.4g) can be derived as usual, and it consists in finding $(\boldsymbol{t},(\boldsymbol{\sigma},\tilde{p}),(\boldsymbol{u},\boldsymbol{\gamma}),p)\in\mathbb{L}^2(\Omega)\times[\mathbb{H}_\Sigma(\mathbf{div},\Omega)\times\mathrm{L}^2(\Omega)]\times[\mathbf{L}^2(\Omega)\times\mathbb{L}^2_{\mathrm{skew}}(\Omega)]\times\mathrm{H}^1_\Sigma(\Omega)$ such that

$$-\int_\Omega \boldsymbol{t}\colon\boldsymbol{\tau}-\int_\Omega \boldsymbol{u}\cdot\mathbf{div}\,\boldsymbol{\tau}-\int_\Omega \boldsymbol{\gamma}\colon\boldsymbol{\tau}=0\quad\forall\boldsymbol{\tau}\in\mathbb{H}_\Sigma(\mathbf{div};\Omega), \tag{3.1a}$$

$$2\mu_s\int_\Omega \boldsymbol{t}\colon\boldsymbol{r}-\int_\Omega \boldsymbol{\sigma}\colon\boldsymbol{r}-\int_\Omega \widetilde{p}\,\mathrm{tr}(\boldsymbol{r})=\beta\int_\Omega \omega\mathrm{tr}(\boldsymbol{r})\quad\forall\boldsymbol{r}\in\mathbb{L}^2(\Omega), \tag{3.1b}$$

$$-\int_\Omega \boldsymbol{\sigma}\colon\boldsymbol{\eta}=0\quad\forall\boldsymbol{\eta}\in\mathbb{L}^2_{\mathrm{skew}}(\Omega), \tag{3.1c}$$

$$-\int_\Omega \boldsymbol{v}\cdot\mathbf{div}\,\boldsymbol{\sigma}=\rho_s\int_\Omega \boldsymbol{f}\cdot\boldsymbol{v}\quad\forall\boldsymbol{v}\in\mathbf{L}^2(\Omega), \tag{3.1d}$$

$$-\left(c_0+\frac{\alpha^2}{\lambda_s}\right)\int_\Omega pq+\frac{\alpha}{\lambda_s}\int_\Omega \widetilde{p}q-\frac{1}{\mu_f}\int_\Omega \boldsymbol{\kappa}\nabla p\cdot\nabla q =\rho_f\int_\Omega \boldsymbol{\kappa}\boldsymbol{g}\cdot\nabla q-\int_\Omega mq\quad\forall q\in\mathrm{H}^1_\Sigma(\Omega), \tag{3.1e}$$

$$-\frac{1}{\lambda_s}\int_\Omega \widetilde{p}\widetilde{q}-\int_\Omega \mathrm{tr}(\boldsymbol{t})\widetilde{q}+\frac{\alpha}{\lambda_s}\int_\Omega p\widetilde{q}=0\quad\forall\widetilde{q}\in\mathrm{L}^2(\Omega). \tag{3.1f}$$

In order to define a weak formulation for problem (2.4h), we remark that the analysis of fixed-point operators (cf. section 3.1) requires that we are able to control the expression

$$\int_\Omega (D(\widetilde{\boldsymbol{\sigma}})-D(\boldsymbol{\sigma}))\nabla\omega\cdot\nabla\widetilde{\omega}, \tag{3.2}$$

where $\boldsymbol{\sigma},\widetilde{\boldsymbol{\sigma}}\in\mathbb{H}_\Sigma(\mathbf{div},\Omega)$ and ω and $\widetilde{\omega}$ are generic scalar fields in suitable spaces. Then, from the Lipschitz continuity of D (cf. (3.6)) together with Cauchy–Schwarz and Hölder inequalities, it can be deduced that

$$\left|\int_\Omega (D(\widetilde{\boldsymbol{\sigma}})-D(\boldsymbol{\sigma}))\nabla\widehat{\omega}\cdot\nabla\widetilde{\omega}\right|\le d_3\|\widetilde{\boldsymbol{\sigma}}-\boldsymbol{\sigma}\|_{\mathbb{L}^2(\Omega)}\|\nabla\omega\|_{\mathbf{L}^{2p}(\Omega)}\|\nabla\widetilde{\omega}\|_{\mathbf{L}^{2q}(\Omega)}, \tag{3.3}$$

where p and q are conjugate exponents (that is, $1/p+1/p'=1$). Then, bearing in mind that a suitable bounding of the expression $\|\nabla\widetilde{\omega}\|_{\mathbf{L}^{2q}(\Omega)}$ (for a particular $\widetilde{\omega}$) will be stipulated later, (3.3) suggests to look for $\omega\in W^{1,r}(\Omega)$, with $r:=2p$. The specific choice of r will be discussed later on, but for the moment let us denote s as its conjugate. The sought variational formulation for (2.4i) now reads as follows: find $\omega\in W^{1,r}_0(\Omega)$ such that

$$\int_\Omega \phi\omega\theta+\int_\Omega D(\boldsymbol{\sigma})\nabla\omega\cdot\nabla\theta=\int_\Omega \ell\phi\theta\quad\forall\theta\in W^{1,s}_0(\Omega). \tag{3.4}$$

Moreover, the unknown ω works as a coupling variable, appearing on the right-hand side of (3.1b). Therefore we should control this term according to the chosen functional setting. Directly from Cauchy–Schwarz and Hölder inequalities and the Sobolev embedding $\mathrm{W}^{1,r}_0(\Omega)\hookrightarrow\mathrm{L}^{\frac{dr}{d-r}}(\Omega)$ we get

$$\beta\int_\Omega \omega\mathrm{tr}(\boldsymbol{r})\le\beta C_H\|\omega\|_{\mathrm{W}^{1,r}(\Omega)}\|\boldsymbol{r}\|_{\mathrm{L}^2(\Omega)}, \tag{3.5}$$

where $C_H>0$ is a constant depending on d, $|\Omega|$ and r. We further assume that $\boldsymbol{\kappa}$ is uniformly bounded and positive definite and that $D(\boldsymbol{\sigma})$ is of class C^1, uniformly

positive definite, and Lipschitz continuous, and this satisfies a particular bounding property: There exist positive constants κ_1, κ_2, and d_1, d_2, d_3, d_4, d_5 such that

$$\kappa_1|\boldsymbol{v}|^2 \le \boldsymbol{v}^{\mathrm{t}}\kappa(\cdot)\boldsymbol{v} \le \kappa_2|\boldsymbol{v}|^2,\ d_1|\boldsymbol{v}|^2 \le \boldsymbol{v}^{\mathrm{t}}D(\cdot)\boldsymbol{v} \le d_2|\boldsymbol{v}|^2, \tag{3.6}$$
$$|D(\boldsymbol{\sigma}) - D(\boldsymbol{\zeta})| \le d_3|\boldsymbol{\sigma} - \boldsymbol{\zeta}|,\ d_4 \le |D(\boldsymbol{\zeta})| \le d_5$$

$\forall \boldsymbol{v} \in \mathbb{R}^d$ and $\forall \boldsymbol{\sigma}, \boldsymbol{\zeta} \in \mathbb{R}^{d\times d}$. Next, we regroup unknowns and spaces in (3.1e)–(3.1b) as follows:

$$\vec{\boldsymbol{\sigma}} := (\boldsymbol{\sigma}, \widetilde{p}),\ \vec{\boldsymbol{\tau}} := (\boldsymbol{\tau}, \widetilde{q}),\ \vec{\boldsymbol{u}} := (\boldsymbol{u}, \boldsymbol{\gamma}),\quad \vec{\boldsymbol{v}} := (\boldsymbol{v}, \boldsymbol{\eta}),\ \mathbf{X} := \mathbb{H}_{\Sigma}(\mathbf{div}; \Omega) \times \mathrm{L}^2(\Omega),$$
$$\mathbf{M} := \mathbf{L}^2(\Omega) \times \mathbb{L}^2_{\mathrm{skew}}(\Omega).$$

Then, given $(H_\omega, F, G, J) \in \mathbb{L}^2(\Omega)' \times \mathbf{M}' \times \mathrm{H}^1_{\Sigma}(\Omega)' \times \mathrm{W}^{1,s}_0(\Omega)'$, we seek $(\boldsymbol{t}, \vec{\boldsymbol{\sigma}}, \vec{\boldsymbol{u}}, p, \omega) \in \mathbb{L}^2(\Omega) \times \mathbf{X} \times \mathbf{M} \times \mathrm{H}^1_{\Sigma}(\Omega) \times \mathrm{W}^{1,r}_0(\Omega)$ such that

$$[A(\boldsymbol{t}), \boldsymbol{r}] + [B^*(\vec{\boldsymbol{\sigma}}), \boldsymbol{r}] = [H_\omega, \boldsymbol{r}], \tag{3.7a}$$
$$[B(\boldsymbol{t}), \vec{\boldsymbol{\tau}}] - [C(\vec{\boldsymbol{\sigma}}), \vec{\boldsymbol{\tau}}] + [B_1^*(\vec{\boldsymbol{u}}), \vec{\boldsymbol{\tau}}] + [B_2^*(p), \vec{\boldsymbol{\tau}}] = \mathrm{O}, \tag{3.7b}$$
$$[B_1(\vec{\boldsymbol{\sigma}}), \vec{\boldsymbol{v}}] = [F, \vec{\boldsymbol{v}}], \tag{3.7c}$$
$$[B_2(\vec{\boldsymbol{\sigma}}), q] - [D(p), q] = [G, q], \tag{3.7d}$$
$$[\mathscr{A}_{\boldsymbol{\sigma}}(\omega), \theta] = [J, \theta] \tag{3.7e}$$

$\forall (\boldsymbol{r}, \vec{\boldsymbol{\tau}}, \vec{\boldsymbol{v}}, q, \theta) \in \mathbb{L}^2(\Omega) \times \mathbf{X} \times \mathbf{M} \times \mathrm{H}^1_{\Sigma}(\Omega) \times \mathrm{W}^{1,s}_0(\Omega)$, where the linear bounded operators $A : \mathbb{L}^2(\Omega) \to \mathbb{L}^2(\Omega)'$, $C : \mathbf{X} \to \mathbf{X}'$, $B : \mathbb{L}^2(\Omega) \to \mathbf{X}'$, $B_1 : \mathbf{X} \to \mathbf{M}'$, $B_2 : \mathbf{X} \to \mathrm{H}^1_{\Sigma}(\Omega)'$, $D : \mathrm{H}^1_{\Sigma}(\Omega) \to \mathrm{H}^1_{\Sigma}(\Omega)'$, $B^* : \mathbf{X} \to \mathbb{L}^2(\Omega)'$, $B_1^* : \mathbf{M} \to \mathbf{X}'$, $B_2^* : \mathrm{H}^1_{\Sigma}(\Omega) \to \mathbf{X}'$, and $\mathscr{A}_{\boldsymbol{\sigma}} : \mathrm{W}^{1,r}_0(\Omega) \to \mathrm{W}^{1,s}_0(\Omega)'$ are defined as

$$[A(\boldsymbol{t}), \boldsymbol{r}] := 2\mu_s \int_\Omega \boldsymbol{t} : \boldsymbol{r}, \tag{3.8a}$$
$$[B(\boldsymbol{r}), \vec{\boldsymbol{\tau}}] := -\int_\Omega \boldsymbol{\tau} : \boldsymbol{r} - \int_\Omega \widetilde{q}\,\mathrm{tr}(\boldsymbol{r}), \tag{3.8b}$$
$$[B_1(\vec{\boldsymbol{\tau}}), \vec{\boldsymbol{v}}] := -\int_\Omega \boldsymbol{v} \cdot \mathbf{div}\,\boldsymbol{\tau} - \int_\Omega \boldsymbol{\eta} : \boldsymbol{\tau}, \tag{3.8c}$$
$$[C(\vec{\boldsymbol{\sigma}}), \vec{\boldsymbol{\tau}}] := \frac{1}{\lambda_s} \int_\Omega \widetilde{p}\,\widetilde{q}, \tag{3.8d}$$
$$[B_2(\vec{\boldsymbol{\tau}}), q] := \frac{\alpha}{\lambda_s} \int_\Omega \widetilde{q} q, \tag{3.8e}$$
$$[D(p), q] := \left(c_0 + \frac{\alpha^2}{\lambda_s}\right) \int_\Omega pq + \frac{1}{\mu_f} \int_\Omega \boldsymbol{\kappa} \nabla p \cdot \nabla q, \tag{3.8f}$$
$$[\mathscr{A}_{\boldsymbol{\sigma}}(\omega), \theta] := \int_\Omega \phi\omega\theta + \int_\Omega D(\boldsymbol{\sigma}) \nabla\omega \cdot \nabla\theta, \tag{3.8g}$$
$$[H_\omega, \boldsymbol{r}] := \beta \int_\Omega \omega\,\mathrm{tr}(\boldsymbol{r}), \tag{3.8h}$$
$$[F, \vec{\boldsymbol{v}}] := \rho_s \int_\Omega \boldsymbol{f} \cdot \boldsymbol{v}, \tag{3.8i}$$
$$[G, q] := -\int_\Omega mq + \rho_f \int_\Omega \boldsymbol{\kappa} \boldsymbol{g} \cdot \nabla q, \tag{3.8j}$$
$$[J, \theta] := \int_\Omega \ell\phi\theta \tag{3.8k}$$

for each $\boldsymbol{t},\boldsymbol{r}\in\mathbb{L}^2(\Omega)$, $\vec{\boldsymbol{\sigma}},\vec{\boldsymbol{\tau}}\in\mathbf{X}$, $\vec{\boldsymbol{u}},\vec{\boldsymbol{v}}\in\mathbf{M}$, $p,q\in\mathrm{H}^1_\Sigma(\Omega)$, $\omega\in\mathrm{W}_0^{1,r}(\Omega)$, and $\theta\in\mathrm{W}_0^{1,s}(\Omega)$. The symbol O stands here for the null functional, and $[\cdot,\cdot]$ denotes the duality pairing induced by the operators and functionals.

3.1. Fixed-point-strategy. In this section, we utilize a fixed-point strategy to prove that (3.7a)–(3.7e) is well-posed. Let $\mathbf{S}:\mathrm{W}_0^{1,r}(\Omega)\to\mathbb{L}^2(\Omega)\times\mathbf{X}\times\mathbf{M}\times\mathrm{H}^1_\Sigma(\Omega)$ be the operator defined by

$$\begin{aligned}\mathbf{S}(\omega)&:=(\mathbf{S}_1(\omega),(\mathbf{S}_2(\omega),\mathbf{S}_3(\omega)),(\mathbf{S}_4(\omega),\mathbf{S}_5(\omega)),\mathbf{S}_6(\omega))\\&=(\boldsymbol{t},(\boldsymbol{\sigma},\widetilde{p}),(\boldsymbol{u},\boldsymbol{\gamma}),p)\in\mathbb{L}^2(\Omega)\times\mathbf{X}\times\mathbf{M}\times\mathrm{H}^1_\Sigma(\Omega),\end{aligned}$$

where $(\boldsymbol{t},(\boldsymbol{\sigma},\widetilde{p}),(\boldsymbol{u},\boldsymbol{\gamma}),p)$ is the unique solution of (3.7a)–(3.7d) with ω given. In turn, we let $\widetilde{\mathbf{S}}:\mathbb{H}_\Sigma(\mathbf{div},\Omega)\to\mathrm{W}_0^{1,r}(\Omega)$ be the operator

$$\widetilde{\mathbf{S}}(\boldsymbol{\sigma}):=\omega\quad\forall\,\boldsymbol{\sigma}\in\mathbb{H}_\Sigma(\mathbf{div},\Omega),$$

where ω is the unique solution of (3.7e) with $\boldsymbol{\sigma}$ given. Then, we define $\mathbf{T}:\mathrm{W}_0^{1,r}(\Omega)\to\mathrm{W}_0^{1,r}(\Omega)$ as

$$\mathbf{T}(\omega):=\widetilde{\mathbf{S}}(\mathbf{S}_2(\omega))\quad\forall\,\omega\in\mathrm{W}_0^{1,r}(\Omega)$$

and realize that solving (3.7a)–(3.7e) is equivalent to finding $\omega\in\mathrm{W}_0^{1,r}(\Omega)$ such that

$$\mathbf{T}(\omega)=\omega. \tag{3.9}$$

3.2. Well-posedness of the uncoupled problems. We analyze the solvability of problems defining $\mathbf{S}$ and $\widetilde{\mathbf{S}}$. In view of the analysis of section 5 and Lemma 3.9 below, the well-posedness and stability of the uncoupled problem related with the operator $\mathbf{S}$ for a given $\omega\in\mathrm{W}_0^{1,r}(\Omega)$ will be developed considering generic functionals $\widetilde{H}_\omega,\widetilde{F}_1,\widetilde{F}$, and $\widetilde{G}$, instead of H_ω,O,F and G, respectively, in (3.7a)–(3.7d). We begin by investigating the well-posedness of this uncoupled problem. First, we recall from [9] the decomposition

$$\mathbb{H}(\mathbf{div},\Omega)=\mathbb{H}_0(\mathbf{div},\Omega)\oplus\mathbb{R}\mathbb{I},\quad\text{with}\quad\mathbb{H}_0(\mathbf{div},\Omega):=\left\{\boldsymbol{\tau}\in\mathbb{H}(\mathbf{div},\Omega):\ \int_\Omega\mathrm{tr}(\boldsymbol{\tau})=0\right\}.$$

That is, for each $\boldsymbol{\tau}\in\mathbb{H}(\mathbf{div},\Omega)$ there exist unique

$$\boldsymbol{\tau}_0:=\boldsymbol{\tau}-\left\{\frac{1}{d|\Omega|}\int_\Omega\mathrm{tr}(\boldsymbol{\tau})\right\}\mathbb{I}\in\mathbb{H}_0(\mathbf{div},\Omega)\quad\text{and}\quad\hat{d}:=\frac{1}{d|\Omega|}\int_\Omega\mathrm{tr}(\boldsymbol{\tau})\in\mathbb{R} \tag{3.10}$$

such that $\boldsymbol{\tau}=\boldsymbol{\tau}_0+\hat{d}\mathbb{I}$. Moreover, we recall the following results which will be useful in the forthcoming analysis. We remit to [22, Lemma 2.3] and [22, Lemma 2.4], respectively, for further details.

LEMMA 3.1. *There exists $c_1>0$, depending only on Ω, such that*

$$c_1\|\boldsymbol{\tau}_0\|^2_{\mathbb{L}^2(\Omega)}\leq\|\boldsymbol{\tau}^{\mathrm{dev}}\|^2_{\mathbb{L}^2(\Omega)}+\|\mathbf{div}(\boldsymbol{\tau})\|^2_{\mathbb{L}^2(\Omega)}\quad\forall\,\boldsymbol{\tau}\in\mathbb{H}(\mathbf{div},\Omega), \tag{3.11}$$

where $\boldsymbol{\tau}^{\mathrm{dev}}$ denotes the deviatoric part of the tensor $\boldsymbol{\tau}$.

LEMMA 3.2. *There exists $c_2 > 0$, depending only on Σ and Ω, such that*

$$c_2\|\boldsymbol{\tau}\|^2_{\mathbb{H}(\mathbf{div},\Omega)} \leq \|\boldsymbol{\tau}_0\|^2_{\mathbb{H}(\mathbf{div},\Omega)} \quad \forall\, \boldsymbol{\tau} \in \mathbb{H}_\Sigma(\mathbf{div},\Omega). \tag{3.12}$$

On the other hand, we can notice that the kernel of B_1 is given by

$$\mathbb{V} := \{\vec{\boldsymbol{\tau}} \in \mathbf{X} : [B_1(\vec{\boldsymbol{\tau}}), \vec{\boldsymbol{v}}] = 0 \ \forall\, \vec{\boldsymbol{v}} \in \mathbf{M}\} = \left\{\vec{\boldsymbol{\tau}} \in \mathbf{X} : \mathbf{div}\,\boldsymbol{\tau} = 0 \text{ and } \boldsymbol{\tau} = \boldsymbol{\tau}^{\mathrm{t}} \text{ in } \Omega\right\}.$$

The following two results will serve to establish the inf-sup conditions for B and B_1 (cf. (3.8b), (3.8c)).

LEMMA 3.3. *There exists $\beta_1 > 0$ such that*

$$\sup_{\vec{\boldsymbol{\tau}} \in \mathbf{X}\setminus\{\mathbf{0}\}} \frac{[B_1(\vec{\boldsymbol{\tau}}), \vec{\boldsymbol{v}}]}{\|\vec{\boldsymbol{\tau}}\|_{\mathbf{X}}} \geq \hat{\beta}_1 \|\vec{\boldsymbol{v}}\|_{\mathbf{M}} \quad \forall\, \vec{\boldsymbol{v}} \in \mathbf{M}.$$

Proof. The (equivalent) surjectivity of B_1 follows as a slight modification to the proof of [21, section 2.4.3]. ∎

LEMMA 3.4. *There exists $\beta > 0$ such that*

$$\sup_{\boldsymbol{r} \in \mathbb{L}^2(\Omega)\setminus\{\mathbf{0}\}} \frac{[B(\boldsymbol{r}), \vec{\boldsymbol{\tau}}]}{\|\boldsymbol{r}\|_{\mathbb{L}^2(\Omega)}} \geq \hat{\beta}\|\vec{\boldsymbol{\tau}}\|_{\mathbf{X}} \quad \forall\, \vec{\boldsymbol{\tau}} \in \mathbb{V}. \tag{3.13}$$

Proof. It follows by using (3.11) and (3.12). For more details see [22, Lemma 2.5]. ∎

Before analyzing (3.7a)–(3.7d), we study the reduced problem: For each $\omega \in \mathrm{W}^{1,r}_0(\Omega)$, find $(\hat{\boldsymbol{t}}, \hat{\tilde{\boldsymbol{\sigma}}}, \hat{p}) \in \mathbb{L}^2(\Omega) \times \mathbb{V} \times \mathrm{H}^1_\Sigma(\Omega)$ such that

$$[A(\hat{\boldsymbol{t}}), \boldsymbol{r}] + [B^*(\hat{\tilde{\boldsymbol{\sigma}}}), \boldsymbol{r}] = [\widetilde{H}_\omega, \boldsymbol{r}], \tag{3.14a}$$

$$[B(\hat{\boldsymbol{t}}), \vec{\boldsymbol{\tau}}] - [C(\hat{\tilde{\boldsymbol{\sigma}}}), \vec{\boldsymbol{\tau}}] + [B_2^*(\hat{p}), \vec{\boldsymbol{\tau}}] = [\widetilde{F}_1, \vec{\boldsymbol{\tau}}], \tag{3.14b}$$

$$[B_2(\hat{\tilde{\boldsymbol{\sigma}}}), q] - [D(\hat{p}), q] = [\widetilde{G}, q] \tag{3.14c}$$

$\forall (\boldsymbol{r}, \vec{\boldsymbol{\tau}}, q) \in \mathbb{L}^2(\Omega) \times \mathbb{V} \times \mathrm{H}^1_\Sigma(\Omega)$, where $\hat{\tilde{\boldsymbol{\sigma}}} := (\hat{\boldsymbol{\sigma}}, \hat{\tilde{p}})$ and $\widetilde{H}_\omega, \widetilde{F}_1$ and $\widetilde{G}$ are the generic functionals mentioned at the beginning of section 3.2. The unique solvability of (3.14a)–(3.14c) proceeds using Fredholm's alternative. Let us recast (3.14a)–(3.14c) with ω given as the following equivalent operator problem: find $\vec{\boldsymbol{t}} := (\hat{\boldsymbol{t}}, \hat{\tilde{\boldsymbol{\sigma}}}, \hat{p}) \in \mathbf{H} := \mathbb{L}^2(\Omega) \times \mathbb{V} \times \mathrm{H}^1_\Sigma(\Omega)$ such that

$$(\mathcal{S} + \mathcal{T})\vec{\boldsymbol{t}} = \mathcal{F}, \tag{3.15}$$

where the linear operators $\mathcal{S}, \mathcal{T} : \mathbf{H} \to \mathbf{H}^*$ and $\mathcal{F} \in \mathbf{H}^*$ are defined, $\forall \vec{\boldsymbol{r}} := (\boldsymbol{r}, \vec{\boldsymbol{\tau}}, q) \in \mathbf{H}$, as

$$[\mathcal{S}(\vec{\boldsymbol{t}}), \vec{\boldsymbol{r}}] := [A(\hat{\boldsymbol{t}}), \boldsymbol{r}] + [B^*(\hat{\tilde{\boldsymbol{\sigma}}}), \boldsymbol{r}] - [B(\hat{\boldsymbol{t}}), \vec{\boldsymbol{\tau}}] + [C(\hat{\tilde{\boldsymbol{\sigma}}}), \vec{\boldsymbol{\tau}}] + [D(\hat{p}), q],$$
$$[\mathcal{T}(\vec{\boldsymbol{t}}), \vec{\boldsymbol{r}}] := -[B_2^*(\hat{p}), \vec{\boldsymbol{\tau}}] - [B_2(\hat{\tilde{\boldsymbol{\sigma}}}), q], \qquad [\mathcal{F}, \vec{\boldsymbol{r}}] := [\widetilde{H}_\omega, r] - [\widetilde{F}_1, \vec{\boldsymbol{\tau}}] - [\widetilde{G}, q].$$

The three upcoming lemmas establish that $\mathcal{S}$ is invertible, $\mathcal{T}$ is compact, and $\mathcal{S} + \mathcal{T}$ is injective. Fredholm's theory will yield the well-posedness of (3.15) and, equivalently, that of (3.14a)–(3.14c), with $\omega \in \mathrm{W}^{1,r}_0(\Omega)$ given.

LEMMA 3.5. *The operator* $\mathcal{S}:\mathbf{H}\to\mathbf{H}^*$ *is invertible.*

Asserting the invertibility of $\mathcal{S}$ is equivalent to proving the unique solvability of the following uncoupled problems: find $(\hat{\boldsymbol{t}},\hat{\vec{\boldsymbol{\sigma}}})\in\mathbb{L}^2(\Omega)\times\mathbb{V}$ such that

$$[A(\hat{\boldsymbol{t}}),\boldsymbol{r}]+[B^*(\hat{\vec{\boldsymbol{\sigma}}}),\boldsymbol{r}]=[F_\omega,\boldsymbol{r}] \qquad \forall\,\boldsymbol{r}\in\mathbb{L}^2(\Omega), \tag{3.16a}$$

$$[B(\hat{\boldsymbol{t}}),\vec{\boldsymbol{\tau}}]-[C(\hat{\vec{\boldsymbol{\sigma}}}),\vec{\boldsymbol{\tau}}]=[F_{\mathbf{X}},\vec{\boldsymbol{\tau}}] \qquad \forall\,\vec{\boldsymbol{\tau}}\in\mathbb{V} \tag{3.16b}$$

and find $\hat{p}\in\mathrm{H}^1_\Sigma(\Omega)$ such that

$$[D(\hat{p}),q]=[F_H,q] \quad \forall\,q\in\mathrm{H}^1_\Sigma(\Omega), \tag{3.17}$$

where, defining $\mathcal{F}:=(\mathcal{F}_\omega,\mathcal{F}_{\mathbf{X}},\mathcal{F}_H)$, the functionals $F_\omega,F_{\mathbf{X}}$, and F_H are the ones induced by the operators $\mathcal{F}_\omega,\mathcal{F}_{\mathbf{X}},\mathcal{F}_H$, respectively. The unique solution of (3.17) simply follows by the Lax–Milgram lemma. In turn, for (3.16a)–(3.16b), we verify the conditions in the linear version of [25, Lemma 2.1]. We first note that

$$[A(\boldsymbol{r}),\boldsymbol{r}]=2\mu_s\|\boldsymbol{r}\|^2_{\mathbb{L}^2(\Omega)} \quad \forall\,\boldsymbol{r}\in\mathbb{L}^2(\Omega), \tag{3.18}$$

which means that the operator A is elliptic on $\mathbb{L}^2(\Omega)$. Moreover, we observe that

$$[C(\vec{\boldsymbol{\tau}}),\vec{\boldsymbol{\tau}}]=\frac{1}{\lambda_s}\|\widetilde{q}\|^2_{\mathrm{L}^2(\Omega)}\geq 0 \quad \forall\,\vec{\boldsymbol{\tau}}\in\mathbb{V}, \tag{3.19}$$

which shows that C is semipositive definite on $\mathbb{V}$. In this way, having in mind (3.18), (3.19), and the inf-sup condition for B given by Lemma 3.4, we simply apply [25, Lemma 2.1] and obtain the desired result.

LEMMA 3.6. *The operator* $\mathcal{T}:\mathbf{H}\to\mathbf{H}^*$ *is compact.*

Proof. Let us to define the operator $\mathbb{B}:\mathrm{L}^2(\Omega)\to\mathrm{H}^1_\Sigma(\Omega)$ as

$$\langle\mathbb{B}(\widetilde{q}),q\rangle_{\mathrm{L}^2(\Omega)}:=\frac{\alpha}{\lambda_s}\int_\Omega\widetilde{q}q \quad \forall\,\widetilde{q}\in\mathrm{L}^2(\Omega)\,\forall\,q\in\mathrm{H}^1_\Sigma(\Omega),$$

where $\langle\cdot,\cdot\rangle_{\mathrm{L}^2(\Omega)}$ stands for the $\mathrm{L}^2(\Omega)$-inner product. Then, thanks to the compactness of the adjoint operator $\mathbb{B}^*$ (see [42, Lemma 2.2]), we deduce that the following operator is also compact:

$$\mathcal{T}(\vec{\boldsymbol{t}})=(\mathbf{0},(\mathbf{0},\mathbb{B}(\hat{\widetilde{p}})),\mathbb{B}^*(\hat{p})).$$

∎

LEMMA 3.7. *The operator* $(\mathcal{S}+\mathcal{T}):\mathbf{H}\to\mathbf{H}^*$ *is injective.*

Proof. It is sufficient to show that the unique solution of the homogeneous problem of (3.14a)–(3.14c) is the null operator in $\mathbf{H}$. Thus, we consider $\widetilde{H}_\omega=\widetilde{F}_1=\widetilde{G}=0$ in (3.14a)–(3.14c), and then, taking $\boldsymbol{r}=\hat{\boldsymbol{t}}$, and $\vec{\boldsymbol{\tau}}=\hat{\vec{\boldsymbol{\sigma}}}$, in (3.14a), and (3.14b), respectively, and applying elementary computations, we obtain

$$2\mu_s\|\hat{\boldsymbol{t}}\|^2_{\mathbb{L}^2(\Omega)}+\frac{1}{\lambda_s}\|\hat{\widetilde{p}}\|^2_{\mathrm{L}^2(\Omega)}-\frac{\alpha}{\lambda_s}\|\hat{\widetilde{p}}\|_{\mathrm{L}^2(\Omega)}\|\hat{p}\|_{\mathrm{H}^1(\Omega)}\leq 0. \tag{3.20}$$

In turn, choosing $q=\hat{p}$ in (3.14c), we have

$$\min\left\{c_0,\frac{\kappa_1}{\mu_f}\right\}\|\hat{p}\|^2_{\mathrm{H}^1(\Omega)}+\frac{\alpha^2}{\lambda_s}\|\hat{p}\|^2_{\mathrm{L}^2(\Omega)}-\frac{\alpha}{\lambda_s}\|\hat{\widetilde{p}}\|_{\mathrm{L}^2(\Omega)}\|\hat{p}\|_{\mathrm{H}^1(\Omega)}\leq 0. \tag{3.21}$$

Thus, by adding (3.20) and (3.21) and applying Young's inequality, we readily obtain $\|\hat{\boldsymbol{t}}\|_{\mathbb{L}^2(\Omega)} = \|\hat{p}\|_{\mathrm{H}^1(\Omega)} = 0$. On the other hand, from Lemma 3.4 and using (3.14a), we get

$$\hat{\beta}\|\hat{\boldsymbol{\sigma}}\|_{\mathbf{X}} \leq \sup_{\substack{\boldsymbol{r}\in\mathbb{L}^2(\Omega)\\ \boldsymbol{r}\neq 0}} \frac{[B(\boldsymbol{r}),\hat{\boldsymbol{\sigma}}]}{\|\boldsymbol{r}\|_{\mathbb{L}^2(\Omega)}} = \sup_{\substack{\boldsymbol{r}\in\mathbb{L}^2(\Omega)\\ \boldsymbol{r}\neq 0}} \frac{-[A(\hat{\boldsymbol{t}}),\boldsymbol{r}]}{\|\boldsymbol{r}\|_{\mathbb{L}^2(\Omega)}} \leq 2\mu_s\|\hat{\boldsymbol{t}}\|_{\mathbb{L}^2(\Omega)},$$

from which we deduce that $\|\hat{\boldsymbol{\sigma}}\|_{\mathbf{X}} = 0$, concluding the proof. ∎

As announced above, thanks to Lemmas 3.5, 3.6, and 3.7 and Fredholm's alternative [47, Theorem 8.2], we deduce the existence of a unique solution to (3.14a)–(3.14c), again, with a given $\omega \in \mathrm{W}_0^{1,r}(\Omega)$. We complement the above result with the stability of (3.14a)–(3.14c) for a given $\omega \in \mathrm{W}_0^{1,r}(\Omega)$.

LEMMA 3.8. *For each $\omega \in \mathrm{W}_0^{1,r}(\Omega)$, there exists a constant $\hat{C} > 0$ independent of λ_s such that*

$$\|\hat{\boldsymbol{t}}\|_{\mathbb{L}^2(\Omega)} + \|\hat{\boldsymbol{\sigma}}\|_{\mathbf{X}} + \|\hat{p}\|_{\mathrm{H}^1(\Omega)} \leq \hat{C}\left(\|\widetilde{H}_\omega\|_{\mathbb{L}^2(\Omega)'} + \|\widetilde{F}_1\|_{\mathbf{X}'} + \|\widetilde{G}\|_{\mathrm{H}^1_\Sigma(\Omega)'}\right).$$

Proof. We proceed similarly as in [35, Theorem 2.1] (see also [6, Theorem 4.3.1]) to obtain suitable estimates and then use linearity. Firstly, we assume that $\widetilde{F}_1 = 0$ and bound the solution in terms of $\widetilde{H}_\omega$ and $\widetilde{G}$, and secondly, we assume that $\widetilde{H}_\omega = 0$, $\widetilde{G} = 0$ and deduce an estimate for the solution in terms of $\widetilde{F}_1$.

Step 1: ($\widetilde{F}_1 = 0$). Proceeding exactly as in the proof of Lemma 3.7, the following bounds can be deduced

$$\|\hat{\boldsymbol{t}}\|_{\mathbb{L}^2(\Omega)} + \|\hat{p}\|_{\mathrm{H}^1(\Omega)} \leq C_1\left(\|\widetilde{H}_\omega\|_{\mathbb{L}^2(\Omega)'} + \|\widetilde{G}\|_{\mathrm{H}^1_\Sigma(\Omega)'}\right), \tag{3.22a}$$

$$\begin{aligned}\hat{\beta}\|\hat{\boldsymbol{\sigma}}\|_{\mathbf{X}} &\leq \sup_{\substack{\boldsymbol{r}\in\mathbb{L}^2(\Omega)\\ \boldsymbol{r}\neq 0}} \frac{[B(\boldsymbol{r}),\hat{\boldsymbol{\sigma}}]}{\|\boldsymbol{r}\|_{\mathbb{L}^2(\Omega)}} = \sup_{\substack{\boldsymbol{r}\in\mathbb{L}^2(\Omega)\\ \boldsymbol{r}\neq 0}} \frac{[\widetilde{H}_\omega,\boldsymbol{r}] - [A(\hat{\boldsymbol{t}}),\boldsymbol{r}]}{\|\boldsymbol{r}\|_{\mathbb{L}^2(\Omega)}}\\ &\leq \|\widetilde{H}_\omega\|_{\mathbb{L}^2(\Omega)'} + 2\mu_s\|\hat{\boldsymbol{t}}\|_{\mathbb{L}^2(\Omega)},\end{aligned} \tag{3.22b}$$

where C_1 is a constant independent of λ_s. Then the desired estimate follows from (3.22a) and (3.22b).

Step 2: ($\widetilde{H}_\omega = 0$ and $\widetilde{G} = 0$). We define

$$\begin{aligned}[S(\hat{\boldsymbol{\sigma}},\hat{p}),(\vec{\boldsymbol{\tau}},q)] &:= [C(\hat{\boldsymbol{\sigma}}),\vec{\boldsymbol{\tau}}] - [B_2^*(\hat{p}),\vec{\boldsymbol{\tau}}] - [B_2(\hat{\boldsymbol{\sigma}}),q] + D[(\hat{p}),q]\\ &= \frac{1}{\lambda_s}\int_\Omega(\hat{\widetilde{p}} - \alpha\hat{p})(\hat{\widetilde{q}} - \alpha q) + c_0\int_\Omega \hat{p}q,\end{aligned}$$

and notice, $\forall \hat{\boldsymbol{\sigma}}, \vec{\boldsymbol{\tau}} \in \mathbb{V}$ and $\hat{p}, q \in \mathrm{H}^1_\Sigma(\Omega)$, that

$$\begin{aligned}|[S(\hat{\boldsymbol{\sigma}},\hat{p}),(\vec{\boldsymbol{\tau}},q)]| &\leq [S(\hat{\boldsymbol{\sigma}},\hat{p}),(\hat{\boldsymbol{\sigma}},\hat{p})]^{1/2}[S(\vec{\boldsymbol{\tau}},q),(\vec{\boldsymbol{\tau}},q)]^{1/2}\\ &= \left(\frac{1}{\lambda_s}\|\hat{\widetilde{p}} - \alpha\hat{p}\|^2_{\mathrm{L}^2(\Omega)} + c_0\|\hat{p}\|^2_{\mathrm{L}^2(\Omega)}\right)^{1/2}\\ &\quad\left(\frac{1}{\lambda_s}\|\hat{\widetilde{q}} - \alpha q\|^2_{\mathrm{L}^2(\Omega)} + c_0\|q\|^2_{\mathrm{L}^2(\Omega)}\right)^{1/2}.\end{aligned} \tag{3.23}$$

Additionally, from the inf-sup condition (3.13) it can be deduced that

$$\sup_{\vec{\boldsymbol{\tau}}\in\mathbb{V}\setminus\{\mathbf{0}\}}\frac{[B(\boldsymbol{r}^{\perp}),\vec{\boldsymbol{\tau}}]}{\|\vec{\boldsymbol{\tau}}\|_{\mathbf{X}}}\geq\hat{\beta}\big\|\boldsymbol{r}^{\perp}\big\|_{\mathbb{L}^2(\Omega)}\quad\forall\,\boldsymbol{r}^{\perp}\in\widetilde{\mathbb{V}}^{\perp},\tag{3.24}$$

where $\widetilde{\mathbb{V}}:=\{\hat{\boldsymbol{r}}\in\mathbb{L}^2(\Omega):[B(\hat{\boldsymbol{r}}),\vec{\boldsymbol{\tau}}]=0\ \forall\,\vec{\boldsymbol{\tau}}\in\mathbb{V}\}$. Now, we let $\hat{\boldsymbol{t}}_0\in\widetilde{\mathbb{V}}$ and $\hat{\boldsymbol{t}}^{\perp}\in\widetilde{\mathbb{V}}^{\perp}$ be such that $\hat{\boldsymbol{t}}=\hat{\boldsymbol{t}}_0+\hat{\boldsymbol{t}}^{\perp}$ and observe from (3.14a)–(3.14c) that there hold

$$[A(\hat{\boldsymbol{t}}),\hat{\boldsymbol{t}}]+[S(\hat{\vec{\boldsymbol{\sigma}}},\hat{p}),(\hat{\vec{\boldsymbol{\sigma}}},\hat{p})]=-\widetilde{F}_1(\hat{\vec{\boldsymbol{\sigma}}}),\tag{3.25a}$$

$$[B(\hat{\boldsymbol{t}}^{\perp}),\vec{\boldsymbol{\tau}}]-[S(\hat{\vec{\boldsymbol{\sigma}}},\hat{p}),(\vec{\boldsymbol{\tau}},q)]=\widetilde{F}_1(\vec{\boldsymbol{\tau}})\quad\forall\,\vec{\boldsymbol{\tau}}\in\mathbb{V}\quad\forall\,q\in\mathrm{H}^1_{\Sigma}(\Omega).\tag{3.25b}$$

Thus, from (3.24) with $\boldsymbol{r}^{\perp}=\hat{\boldsymbol{t}}^{\perp}$, estimate (3.25b), the continuity of $\widetilde{F}_1$, and the bound (3.23), we get

$$\begin{aligned}\hat{\beta}\|\hat{\boldsymbol{t}}^{\perp}\|_{\mathbb{L}^2(\Omega)}&\leq\sup_{\vec{\boldsymbol{\tau}}\in\mathbb{V}\setminus\{\mathbf{0}\}}\frac{[B(\hat{\boldsymbol{t}}^{\perp}),\vec{\boldsymbol{\tau}}]}{\|\vec{\boldsymbol{\tau}}\|_{\mathbf{X}}}=\sup_{\vec{\boldsymbol{\tau}}\in\mathbb{V}\setminus\{\mathbf{0}\}}\frac{\widetilde{F}_1(\vec{\boldsymbol{\tau}})+[S(\hat{\vec{\boldsymbol{\sigma}}},\hat{p}),(\vec{\boldsymbol{\tau}},q)]}{\|\vec{\boldsymbol{\tau}}\|_{\mathbf{X}}}\\&\leq\|\widetilde{F}_1\|_{\mathbf{X}'}+[S(\hat{\vec{\boldsymbol{\sigma}}},\hat{p}),(\hat{\vec{\boldsymbol{\sigma}}},\hat{p})]^{1/2}\sup_{\vec{\boldsymbol{\tau}}\in\mathbb{V}\setminus\{\mathbf{0}\}}\frac{\Big(\frac{1}{\lambda_s}\|\hat{\widetilde{q}}-\alpha q\|^2_{\mathrm{L}^2(\Omega)}+c_0\|q\|^2_{\mathrm{L}^2(\Omega)}\Big)^{1/2}}{\|\vec{\boldsymbol{\tau}}\|_{\mathbf{X}}}.\end{aligned}\tag{3.26}$$

Then, defining

$$C_S:=\sup_{\vec{\boldsymbol{\tau}}\in\mathbb{V}\setminus\{\mathbf{0}\}}\frac{\Big(\frac{1}{\lambda_s}\|\hat{\widetilde{q}}-\alpha q\|^2_{\mathrm{L}^2(\Omega)}+c_0\|q\|^2_{\mathrm{L}^2(\Omega)}\Big)^{1/2}}{\|\vec{\boldsymbol{\tau}}\|_{\mathbf{X}}},$$

which can be seen as a constant independent of λ_s if $\lambda_s\to\infty$, and noticing from (3.25a) that

$$[S(\hat{\vec{\boldsymbol{\sigma}}},\hat{p}),(\hat{\vec{\boldsymbol{\sigma}}},\hat{p})]\leq-\widetilde{F}_1(\hat{\vec{\boldsymbol{\sigma}}}),$$

it can be deduced from (3.26) that

$$\hat{\beta}\|\hat{\boldsymbol{t}}^{\perp}\|_{\mathbb{L}^2(\Omega)}\leq\|\widetilde{F}_1\|_{\mathbf{X}'}+C_S[S(\hat{\vec{\boldsymbol{\sigma}}},\hat{p}),(\hat{\vec{\boldsymbol{\sigma}}},\hat{p})]^{1/2}\leq\|\widetilde{F}_1\|_{\mathbf{X}'}+C_S\|\widetilde{F}_1\|^{1/2}_{\mathbf{X}'}\|\hat{\vec{\boldsymbol{\sigma}}}\|^{1/2}_{\mathbf{X}}.\tag{3.27}$$

Furthermore, taking $\hat{\boldsymbol{t}}_0$ in (3.14a), applying the ellipticity and continuity of A, and recalling (3.10), we easily get

$$\|\hat{\boldsymbol{t}}\|_{\mathbb{L}^2(\Omega)}\leq(1+\widetilde{C}_1)\|\hat{\boldsymbol{t}}^{\perp}\|_{\mathbb{L}^2(\Omega)}.\tag{3.28}$$

In this way, from (3.28), the inf-sup condition (3.13), and (3.14a), it readily follows that

$$\begin{aligned}\|\hat{\vec{\boldsymbol{\sigma}}}\|_{\mathbf{X}}\leq\hat{\beta}^{-1}\sup_{\substack{\boldsymbol{r}\in\mathbb{L}^2(\Omega)\\ \boldsymbol{r}\neq\mathbf{0}}}\frac{[B(\boldsymbol{r}),\hat{\vec{\boldsymbol{\sigma}}}]}{\|\boldsymbol{r}\|_{\mathbb{L}^2(\Omega)}}&=\hat{\beta}^{-1}\sup_{\substack{\boldsymbol{r}\in\mathbb{L}^2(\Omega)\\ \boldsymbol{r}\neq\mathbf{0}}}\frac{-[A(\hat{\boldsymbol{t}}),\boldsymbol{r}]}{\|\boldsymbol{r}\|_{\mathbb{L}^2(\Omega)}}\leq2\mu_s\hat{\beta}^{-1}\|\hat{\boldsymbol{t}}\|_{\mathbb{L}^2(\Omega)}\\&\leq\widetilde{C}_2\|\hat{\boldsymbol{t}}^{\perp}\|_{\mathbb{L}^2(\Omega)},\end{aligned}\tag{3.29}$$

which combined with (3.27) and the Young's inequality yields

$$\|\hat{\boldsymbol{t}}^{\perp}\|_{\mathbb{L}^2(\Omega)}\leq\widetilde{C}_3\|\widetilde{F}_1\|_{\mathbf{X}'}.$$

Therefore, from the latter inequality, (3.28), and (3.29), we derive that

$$\|\hat{\boldsymbol{t}}\|_{\mathbb{L}^2(\Omega)} \leq \widetilde{C}_4 \|\widetilde{F}_1\|_{\mathbf{X}'} \quad \text{and} \quad \|\hat{\vec{\boldsymbol{\sigma}}}\|_{\mathbf{X}} \leq \widetilde{C}_5 \|\widetilde{F}_1\|_{\mathbf{X}'}, \tag{3.30}$$

where $\widetilde{C}_4 > 0$ and $\widetilde{C}_5 > 0$ are constants independent of λ_s. Finally, the ellipticity of D and (3.14c) yield

$$\|\hat{p}\|^2_{\mathrm{H}^1(\Omega)} \leq \widetilde{C}_6 \|\hat{p}\|_{\mathrm{H}^1(\Omega)} \|\hat{\vec{\boldsymbol{\sigma}}}\|_{\mathbf{X}}. \tag{3.31}$$

In this way, the result follows from (3.30) and (3.31) and after applying algebraic manipulations. ∎

Finally, the main result is given next.

LEMMA 3.9. *For each $\omega \in \mathrm{W}_0^{1,r}(\Omega)$ the problem* (3.7a)–(3.7d) *has a unique solution $(\boldsymbol{t}, \vec{\boldsymbol{\sigma}}, \vec{\boldsymbol{u}}, p) \in \mathbb{L}^2(\Omega) \times \mathbf{X} \times \mathbf{M} \times \mathrm{H}^1_\Sigma(\Omega)$. Moreover, there exists $C > 0$ independent of ω and λ_s such that*

$$\|\boldsymbol{t}\|_{\mathbb{L}^2(\Omega)} + \|\vec{\boldsymbol{\sigma}}\|_{\mathbf{X}} + \|\vec{\boldsymbol{u}}\|_{\mathbf{M}} + \|p\|_{\mathrm{H}^1(\Omega)} \leq C \left(\|\widetilde{H}_\omega\|_{\mathbb{L}^2(\Omega)'} + \|\widetilde{F}_1\|_{\mathbf{X}'} + \|\widetilde{F}\|_{\mathbf{M}'} + \|\widetilde{G}\|_{\mathrm{H}^1_\Sigma(\Omega)'} \right). \tag{3.32}$$

Proof. We proceed similarly as in [25, Theorem 2.1]. Recall from [29, Lemma 4.1] that the result given in Lemma 3.3 implies that $B_1 : \mathbb{V}^\perp \to \mathbf{M}'$ and $B_1^* : \mathbf{M} \to \mathbb{V}^\circ$ are isomorphisms with

$$\|B_1\|, \quad \|(B_1^*)^{-1}\| \leq \frac{1}{\hat{\beta}_1}, \tag{3.33}$$

where $\mathbb{V}^\circ$ stands for the set of functionals in $\mathbf{X}$ that vanish on the elements of $\mathbb{V}$. Now, let $\vec{\boldsymbol{\sigma}}_0 := B_1^{-1}(\widetilde{F}) \in \mathbb{V}^\perp$, and notice that by using (3.33) it can be deduced that

$$\|\vec{\boldsymbol{\sigma}}_0\|_{\mathbf{X}} \leq \frac{1}{\beta_1} \|\widetilde{F}\|_{\mathbf{M}'}. \tag{3.34}$$

With this in mind, we define the functionals $\underline{H}_\omega := \widetilde{H}_\omega - B^*(\vec{\boldsymbol{\sigma}}_0)$, $\underline{F} := \widetilde{F}_1 + C(\vec{\boldsymbol{\sigma}}_0)$ and $\underline{G} := \widetilde{G} - B_2(\vec{\boldsymbol{\sigma}}_0)$ and consider the following problem: Find $(\underline{\boldsymbol{t}}, \underline{\vec{\boldsymbol{\sigma}}}, \underline{p}) \in \mathbb{L}^2(\Omega) \times \mathbb{V} \times \mathrm{H}^1_\Sigma(\Omega)$ such that

$$\begin{aligned} [A(\underline{\boldsymbol{t}}), \boldsymbol{r}] + [B^*(\underline{\vec{\boldsymbol{\sigma}}}), \boldsymbol{r}] &= [\underline{H}_\omega, \boldsymbol{r}], \\ [B(\underline{\boldsymbol{t}}), \vec{\boldsymbol{\tau}}] - [C(\underline{\vec{\boldsymbol{\sigma}}}), \vec{\boldsymbol{\tau}}] + [B_2^*(\underline{p}), \vec{\boldsymbol{\tau}}] &= \underline{F}, \vec{\boldsymbol{\tau}}], \\ [B_2(\underline{\vec{\boldsymbol{\sigma}}}), q] - [D(\underline{p}), q] &= [\underline{G}, q] \end{aligned} \tag{3.35}$$

$\forall (\boldsymbol{r}, \vec{\boldsymbol{\tau}}, q) \in \mathbb{L}^2(\Omega) \times \mathbb{V} \times \mathrm{H}^1_\Sigma(\Omega)$, where the involved operators are exactly the ones defining (3.14a)–(3.14c). Therefore, by noticing that $\underline{H}_\omega \in \mathbb{L}^2(\Omega)'$, $\underline{F} \in \mathbb{V}^\circ$, and $\underline{G} \in \mathrm{H}^1_\Sigma(\Omega)'$, we can simply take $\widetilde{H}_\omega$, $\widetilde{F}_1$ and $\widetilde{G}$ in (3.14a)–(3.14c) as $\underline{H}_\omega$, $\underline{F}$, and $\underline{G}$, respectively, and apply Lemma 3.8 to assert the existence and uniqueness of a solution $(\underline{\boldsymbol{t}}, \underline{\vec{\boldsymbol{\sigma}}}, \underline{p}) \in \mathbb{L}^2(\Omega) \times \mathbb{V} \times \mathrm{H}^1_\Sigma(\Omega)$ to problem (3.35).

On the other hand, since $(\underline{F} - B(\underline{\boldsymbol{t}}) + C(\underline{\vec{\boldsymbol{\sigma}}}) - B_2^*(\underline{p})) \in \mathbb{V}^\circ$, we can take $\underline{\vec{\boldsymbol{u}}} := (B_1^*)^{-1}(\underline{F} - B(\underline{\boldsymbol{t}}) + C(\underline{\vec{\boldsymbol{\sigma}}}) - B_2^*(\underline{p})) \in \mathbf{M}$, from which it is clear that

$$[B_1^*(\underline{\vec{\boldsymbol{u}}}), \vec{\boldsymbol{\tau}}] = [\underline{F} - B(\underline{\boldsymbol{t}}) + C(\underline{\vec{\boldsymbol{\sigma}}}) - B_2^*(\underline{p}), \vec{\boldsymbol{\tau}}] \quad \forall\, \vec{\boldsymbol{\tau}} \in \mathbf{X}, \tag{3.36}$$

and therefore,

$$\|\underline{\vec{\boldsymbol{u}}}\|_{\mathbf{M}} \leq \frac{1}{\beta_1} \|\underline{F} - B(\underline{\boldsymbol{t}}) + C(\underline{\vec{\boldsymbol{\sigma}}}) - B_2^*(\underline{p})\|. \tag{3.37}$$

In this manner, noting also that $B_1(\underline{\vec{\boldsymbol{\sigma}}} + \vec{\boldsymbol{\sigma}}_0) = B_1(\vec{\boldsymbol{\sigma}}_0) = \widetilde{F}$, we finally conclude for each $\omega \in \mathrm{W}_0^{1,r}(\Omega)$ that $(\underline{\boldsymbol{t}}, \underline{\vec{\boldsymbol{\sigma}}} + \vec{\boldsymbol{\sigma}}_0, \underline{\vec{\boldsymbol{u}}}, \underline{p}) \in \mathbb{L}^2(\Omega) \times \mathbf{X} \times \mathbf{M} \times \mathrm{H}^1_{\Sigma}(\Omega)$ is a solution of (3.7a)–(3.7d).

Now, for the uniqueness, consider another solution $(\boldsymbol{t}, \vec{\boldsymbol{\sigma}}, \vec{\boldsymbol{u}}, p) \in \mathbb{L}^2(\Omega) \times \mathbf{X} \times \mathbf{M} \times \mathrm{H}^1_{\Sigma}(\Omega)$ of (3.7a)–(3.7d). It is fairly directly seen from (3.7a)–(3.7d) that $(\boldsymbol{t}, \vec{\boldsymbol{\sigma}} - \vec{\boldsymbol{\sigma}}_0, p) \in \mathbb{L}^2(\Omega) \times \mathbb{V} \times \mathrm{H}^1_{\Sigma}(\Omega)$ is also a solution of (3.35), and therefore $(\boldsymbol{t}, \vec{\boldsymbol{\sigma}} - \vec{\boldsymbol{\sigma}}_0, p) = (\underline{\boldsymbol{t}}, \underline{\vec{\boldsymbol{\sigma}}}, \underline{p})$, which together with (3.36) gives $(\boldsymbol{t}, \vec{\boldsymbol{\sigma}}, \vec{\boldsymbol{u}}, p) = (\underline{\boldsymbol{t}}, \underline{\vec{\boldsymbol{\sigma}}} + \vec{\boldsymbol{\sigma}}_0, \underline{\vec{\boldsymbol{u}}}, \underline{p})$.

On the other hand, in order to deduce the stability estimate (3.32) we begin by using (3.37) to obtain

$$\|\vec{\boldsymbol{u}}\|_{\mathbf{M}} \leq \frac{1}{\beta_1} \| - B(\boldsymbol{t}) + C(\vec{\boldsymbol{\sigma}}_0) - B_2^*(p)\|,$$

from which, by using the definitions (3.8d), (3.8e), the inf-sup condition (3.13), and the bound (3.34), we deduce that there exists $\underline{C}_1 > 0$ independent of λ_s such that

$$\|\vec{\boldsymbol{u}}\|_{\mathbf{M}} \leq \underline{C}_1 \left\{ \|\boldsymbol{t}\|_{\mathbb{L}^2(\Omega)} + \frac{1}{\lambda_s} \|\widetilde{F}\|_{\mathbf{M}'} + \frac{\alpha}{\lambda_s} \|p\|_{\mathrm{H}^1(\Omega)} \right\}. \tag{3.38}$$

Moreover, applying Lemma 3.8 to (3.35), we deduce the existence of $\underline{C} > 0$, independent of λ_s, such that

$$\begin{aligned} &\|\boldsymbol{t}\|_{\mathbb{L}^2(\Omega)} + \|\vec{\boldsymbol{\sigma}} - \vec{\boldsymbol{\sigma}}_0\|_{\mathbf{X}} + \|p\|_{\mathrm{H}^1(\Omega)} \\ &\quad \leq \underline{C} \left\{ \|\widetilde{H}_\omega - B^*(\vec{\boldsymbol{\sigma}}_0)\| + \|\widetilde{F}_1 + C(\vec{\boldsymbol{\sigma}}_0)\| + \|\widetilde{G} - B_2(\vec{\boldsymbol{\sigma}}_0)\| \right\}. \end{aligned}$$

Thus, from the definitions in (3.8a), (3.8i), and (3.8j), we proceed as before to get

$$\begin{aligned} &\|\boldsymbol{t}\|_{\mathbb{L}^2(\Omega)} + \|\vec{\boldsymbol{\sigma}}\|_{\mathbf{X}} + \|p\|_{\mathrm{H}^1(\Omega)} \\ &\quad \leq \underline{C}_2 \left\{ \|\widetilde{H}_\omega\|_{\mathbb{L}^2(\Omega)'} + \|\widetilde{F}_1\|_{\mathbf{X}'} + \left(1 + \frac{1}{\lambda_s} + \frac{\alpha}{\lambda_s}\right) \|\widetilde{F}\|_{\mathbf{M}'} + \|\widetilde{G}\|_{\mathrm{H}^1_{\Sigma}(\Omega)'} \right\}, \end{aligned} \tag{3.39}$$

where $\underline{C}_2 > 0$ is independent of λ_s. In this way, replacing (3.39) back into (3.38), we deduce that

$$\begin{aligned} &\|\boldsymbol{t}\|_{\mathbb{L}^2(\Omega)} + \|\vec{\boldsymbol{\sigma}}\|_{\mathbf{X}} + \|\vec{\boldsymbol{u}}\|_{\mathbf{M}} + \|p\|_{\mathrm{H}^1(\Omega)} \\ &\quad \leq \underline{C}_3 \left(1 + \frac{\alpha}{\lambda_s}\right) \left\{ \|\widetilde{H}_\omega\|_{\mathbb{L}^2(\Omega)'} + \|\widetilde{F}_1\|_{\mathbf{X}'} + \left(1 + \frac{2}{\lambda_s} + \frac{\alpha}{\lambda_s}\right) \|\widetilde{F}\|_{\mathbf{M}'} + \|\widetilde{G}\|_{\mathrm{H}^1_{\Sigma}(\Omega)'} \right\}. \end{aligned}$$

Therefore, noting that the constants $1 + \frac{\alpha}{\lambda_s}$ and $1 + \frac{2}{\lambda_s} + \frac{\alpha}{\lambda_s}$ are understood as independent of λ_s in the limit $\lambda_s \to \infty$, we can apply elementary algebraic computations to deduce the existence of a constant C independent of λ_s such that (3.32) holds. ∎

We establish now the well-posedness of the operator $\widetilde{\mathbf{S}}$. Consider the following problem: find $\omega \in \mathrm{W}_0^{1,r}(\Omega)$ such that

$$[A_1(\omega), \theta] + [A_2(\omega), \theta] = [J, \theta] \qquad \forall\, \theta \in \mathrm{W}_0^{1,s}(\Omega), \tag{3.40}$$

where $[J, \theta]$ is defined in (3.8k) and where $[A_1(\widetilde{\omega}), \theta] := \int_\Omega \vartheta \nabla \widetilde{\omega} \cdot \nabla \theta$, and $[A_2(\widetilde{\omega}), \theta] := \int_\Omega \phi \widetilde{\omega} \theta$, with ϑ considered as a real-valued $n \times n$ symmetric matrix satisfying the second and fourth conditions in (3.6) (taking ϑ instead of D) and ϕ defined as in (2.2). Moreover, we recall from [1] (see also [48]) the following results which will be useful in the forthcoming analysis.

LEMMA 3.10. *Let r be such that $2d/(d+1) - \varepsilon < r < 2$ with $\varepsilon > 0$. Then, there exists $\beta_{\mathscr{A}}$ such that problem* (3.40) *with $A_2 = \mathrm{O}$ (the null operator) is well defined, and there holds*

$$\beta_{\mathscr{A}} \|\nabla \widetilde{\omega}\|_{\mathbf{L}^r(\Omega)} \leq \sup_{\theta \in \mathrm{W}^{1,s}(\Omega)\setminus\{\mathbf{0}\}} \frac{\int_\Omega \vartheta \nabla \widetilde{\omega} \cdot \nabla \theta}{\|\nabla \theta\|_{\mathbf{L}^s(\Omega)}} \qquad \forall \widetilde{\omega} \in \mathrm{W}^{1,r}(\Omega). \tag{3.41}$$

Proof. The proof follows from [1, Proposition 3]. ∎

LEMMA 3.11. *Assume that $\beta_{\mathscr{A}}\phi < 1$, and that r satisfies the range given in Lemma* 3.10. *Then, problem* (3.40) *is well-posed, and there holds*

$$\|\nabla \omega\|_{\mathbf{L}^r(\Omega)} \leq \frac{\beta_{\mathscr{A}}^{-1}}{1 - \beta_{\mathscr{A}}^{-1}\phi} \|J\|_{\mathrm{W}_0^{1,r}(\Omega)'}. \tag{3.42}$$

Proof. It follows similarly to the proof of [1, Proposition 4]. In fact, from (3.41) it can be deduced that A_1 is invertible with $\|A_1^{-1}\| \leq \beta_{\mathscr{A}}$. Additionally, it can be noticed that the map A_2 is linear and bounded. Then, problem (3.40) can be rewritten as $(\mathbb{I} + A_1^{-1}A_2)\omega = A_1^{-1}J$. In this way, the boundedness of the maps A_1^{-1} and A_2 combined with the assumption $\beta_{\mathscr{A}}^{-1}\phi < 1$ yield that the $W_0^{1,r}(\Omega)$-norm is bounded by 1. Therefore, by applying [57, Theorem 1.B], we conclude that (3.40) has a unique solution. Finally, the estimate (3.42) can be obtained from the aforementioned modified problem. ∎

We are now in a position to establish the desired result for $\widetilde{\mathbf{S}}$.

LEMMA 3.12. *For each $\boldsymbol{\sigma} \in \mathbb{H}_\Sigma(\mathbf{div}, \Omega)$, the problem* (3.7e) *has a unique solution $\omega := \widetilde{\mathbf{S}}(\boldsymbol{\sigma}) \in \mathrm{W}_0^{1,r}(\Omega)$, and there holds*

$$\|\widetilde{\mathbf{S}}(\boldsymbol{\sigma})\| := \|\omega\|_{\mathrm{W}^{1,r}(\Omega)} \leq \frac{\beta_{\mathscr{A}}^{-1}}{1 - \beta_{\mathscr{A}}^{-1}\phi} \|J\|_{\mathrm{W}_0^{1,r}(\Omega)'}. \tag{3.43}$$

Proof. The proof follows simply as an application of Lemma 3.11. ∎

As $\mathbf{S}$ and $\widetilde{\mathbf{S}}$ are well defined, we can guarantee the well-posedness of the operator $\mathbf{T}$.

3.3. Solvability of the fixed-point problem. With the aim to use the Banach fixed-point theorem on $\mathbf{T}$, in what follows we establish sufficient conditions under which $\mathbf{T}$ maps a closed ball of $\mathrm{W}_0^{1,r}(\Omega)$ into itself. Indeed, from now on we let

$$\mathbf{W} := \left\{ \omega \in \mathrm{W}_0^{1,r}(\Omega) : \ \|\omega\|_{\mathrm{W}^{1,r}(\Omega)} \leq \zeta := \frac{\beta_{\mathscr{A}}^{-1}}{1 - \beta_{\mathscr{A}}^{-1}\phi} \|J\|_{\mathrm{W}_0^{1,r}(\Omega)'} \right\}. \tag{3.44}$$

LEMMA 3.13. *Assume that $\beta_{\mathscr{A}}^{-1}\phi < 1$. For the closed ball $\mathbf{W}$, it holds that $\mathbf{T}(\mathbf{W}) \subseteq \mathbf{W}$.*

Proof. The proof suffices to recall the definition of $\mathbf{T}$ (3.9) and then apply the estimate (3.43). ∎

We now verify the hypotheses of the fixed-point theorem. As a preliminary step, we show the Lipschitz continuity of $\mathbf{S}$.

LEMMA 3.14. *There exists a constant $C_{\mathbf{S}} > 0$ independent of λ_s such that*

$$\|\mathbf{S}(\omega_1) - \mathbf{S}(\omega_2)\| \leq C_{\mathbf{S}} C_H \beta \|\omega_1 - \omega_2\|_{\mathrm{W}^{1,r}(\Omega)} \quad \forall \omega_1, \omega_2 \in \mathrm{W}_0^{1,r}(\Omega),$$

where $C_H > 0$ is the constant given in (3.5).

Proof. Let $(\boldsymbol{t}_1, \vec{\boldsymbol{\sigma}}_1, \vec{\boldsymbol{u}}_1, r_1)$ and $(\boldsymbol{t}_2, \vec{\boldsymbol{\sigma}}_2, \vec{\boldsymbol{u}}_2, p_2)$ be two solutions of the problem (3.7a)–(3.7d), with ω_1 and $\omega_2 \in \mathrm{W}_0^{1,r}(\Omega)$ given such that $\mathbf{S}(\omega_1) := (\boldsymbol{t}_1, \vec{\boldsymbol{\sigma}}_1, \vec{\boldsymbol{u}}_1, r_1)$ and $\mathbf{S}(\omega_2) := (\boldsymbol{t}_2, \vec{\boldsymbol{\sigma}}_2, \vec{\boldsymbol{u}}_2, p_2)$. Then, by applying the linearity of the involved bilinear forms and functionals, we obtain

$$\begin{aligned}
[A(\boldsymbol{t}_1 - \boldsymbol{t}_2), \boldsymbol{r}] + B(\boldsymbol{r}), \vec{\boldsymbol{\sigma}}_1 - \vec{\boldsymbol{\sigma}}_2] &= [H_{\omega_1 - \omega_2}, \boldsymbol{r}], \\
[B(\boldsymbol{t}_1 - \boldsymbol{t}_2), \vec{\boldsymbol{\tau}}] - [C(\vec{\boldsymbol{\tau}}), \vec{\boldsymbol{\sigma}}_1 - \vec{\boldsymbol{\sigma}}_2] + [B_1(\vec{\boldsymbol{\tau}}), \vec{\boldsymbol{u}} - \vec{\boldsymbol{u}_2}] + [B_2(\vec{\boldsymbol{\tau}}), p_1 - p_2] &= 0, \\
[B_1(\vec{\boldsymbol{\sigma}}_1 - \vec{\boldsymbol{\sigma}}_2), \vec{\boldsymbol{v}}] &= 0, \\
[B_2(\vec{\boldsymbol{\sigma}}), q] - [D(p), q] &= 0
\end{aligned}$$

for each $(\boldsymbol{r}, \vec{\boldsymbol{\tau}}, \vec{\boldsymbol{v}}, p) \in \mathbb{L}^2(\Omega) \times \mathbf{X} \times \mathbf{M} \times \mathrm{H}^1_\Sigma(\Omega)$. Proceeding as in the proof of the well-posedness of the decoupled poroelasticity problem, we deduce that

$$\|\mathbf{S}(\omega_1) - \mathbf{S}(\omega_2)\| = \|(\boldsymbol{t}_1, \vec{\boldsymbol{\sigma}}_1, \vec{\boldsymbol{u}}_1, p_1) - (\boldsymbol{t}_2, \vec{\boldsymbol{\sigma}}_2, \vec{\boldsymbol{u}}_2, p_2)\| \leq C_{\mathbf{S}} C_H \beta \|\omega_1 - \omega_2\|_{\mathrm{W}^{1,r}(\Omega)}. \quad \square$$

Now that we have established the previous result, we focus on proving the Lipschitz continuity of $\widetilde{\mathbf{S}}$. To do so, we state a suitable regularity estimate that will be necessary for what follows.

- **(RE)** Assume that $\partial\Omega$ is of class $\mathcal{C}^2$. The Lipschitz continuity of the diffusion operator D in combination with elliptic regularity (cf. [28]) allows us to assert that $\widetilde{\mathbf{S}}(\boldsymbol{\sigma}) = \omega \in W_0^{2,2}(\Omega)$ for each $\boldsymbol{\sigma} \in \mathbb{H}_\Sigma(\mathbf{div}, \Omega)$ and that there is a positive constant C_R such that

$$\|\widetilde{\mathbf{S}}(\boldsymbol{\sigma})\|_{\mathrm{W}^{2,2}(\Omega)} = \|\omega\|_{\mathrm{W}^{2,2}(\Omega)} \leq C_R \|J\|_{\mathrm{L}^2(\Omega)'}. \tag{3.45}$$

  Considering $r < 2$ and utilizing the estimate (3.45), for the case $d = 2$ we can apply the Sobolev embedding $\mathrm{W}_0^{1,r}(\Omega) \hookrightarrow \mathrm{L}^{\frac{2r}{2-r}}(\Omega)$ to deduce that, for every $\boldsymbol{\sigma} \in \mathbb{H}_\Sigma(\mathbf{div}, \Omega)$, we have

$$\begin{aligned}
\|\nabla \widetilde{\mathbf{S}}(\boldsymbol{\sigma})\|_{\mathbf{L}^{\frac{2r}{2-r}}(\Omega)} &= \|\nabla \omega\|_{\mathbf{L}^{\frac{2r}{2-r}}(\Omega)} \leq C_e \|\nabla \omega\|_{\mathbf{W}^{1,r}(\Omega)} \\
&= C_e \|\omega\|_{\mathrm{W}^{2,r}(\Omega)} \leq C_e \|\omega\|_{\mathrm{W}^{2,2}(\Omega)} \leq C_{RE} \|J\|_{\mathrm{L}^2(\Omega)'},
\end{aligned} \tag{3.46}$$

  where C_e represents the best constant in this embedding, and $C_{RE} := C_e C_R$. Note that the Sobolev embedding used in (RE) renders the previous result inapplicable to three dimensions. Nonetheless, to bound a term arising from (3.48) using an estimate similar to (3.46), the approach in [23, 24], which employs an $\mathrm{L}^\infty - \mathrm{L}^2 - \mathrm{L}^2$ argument for (3.48), may still be sufficient. Although there are regularity results giving $\boldsymbol{u} \in \mathbf{H}^2(\Omega)$ for the classical poroelasticity problem (cf. [56]), they are not necessarily relevant to our situation due to the coupling with ω; those results would require $\nabla \omega \in \mathbf{L}^2(\Omega)$ rather than $\nabla \omega \in \mathbf{L}^r(\Omega)$ with $r < 2$ as in our case. In this way, and unlike [23, 24], we do not have that $D(\boldsymbol{\sigma})_{ij} \in \mathcal{C}^{1+\gamma}$ for some $\gamma > 1/2$, and we are unable to apply classical regularity results.

Thus, we only make the assumption of extending (3.46) to three dimensions and proceed next to prove the Lipschitz continuity of $\widetilde{\mathbf{S}}$.

LEMMA 3.15. *Let $d_3, \beta_{\widetilde{\mathbf{S}}}$, and C_{RE} be defined by* (3.6), (3.47), *and* (3.46), *respectively. Then*

$$\|\widetilde{\mathbf{S}}(\boldsymbol{\sigma}) - \widetilde{\mathbf{S}}(\widetilde{\boldsymbol{\sigma}})\| \leq d_3 \beta_{\widetilde{\mathbf{S}}}^{-1} C_{RE} \|J\|_{\mathrm{L}^2(\Omega)'} \|\widetilde{\boldsymbol{\sigma}} - \boldsymbol{\sigma}\|_{\mathbb{L}^2(\Omega)} \quad \forall\, \boldsymbol{\sigma}, \widetilde{\boldsymbol{\sigma}} \in \mathbb{H}_\Sigma(\mathbf{div}, \Omega).$$

Proof. Given $\boldsymbol{\sigma}$ and $\widetilde{\boldsymbol{\sigma}} \in \mathbb{H}_\Sigma(\mathbf{div},\Omega)$, we let ω and $\widetilde{\omega}$ be two solutions of problem (3.7e). That is, $\omega := \widetilde{\mathbf{S}}(\boldsymbol{\sigma})$ and $\widetilde{\omega} := \widetilde{\mathbf{S}}(\widetilde{\boldsymbol{\sigma}})$. Then, thanks to [18, Theorem 2.6] we can ensure that there exists $\beta_{\widehat{\mathbf{S}}} > 0$ such that

$$\beta_{\widehat{\mathbf{S}}} \|\nabla \widehat{\omega}\|_{\mathbf{L}^r(\Omega)} \leq \sup_{\theta \in \mathrm{W}^{1,s}(\Omega)\setminus\{0\}} \frac{[\mathscr{A}_{\boldsymbol{\sigma}}(\widehat{\omega}),\theta]}{\|\nabla\theta\|_{\mathbf{L}^s(\Omega)}} \qquad \forall\, \widehat{\omega} \in \mathrm{W}^{1,r}(\Omega). \tag{3.47}$$

In particular, for $(\omega - \widetilde{\omega}) \in \mathrm{W}^{1,r}_0(\Omega)$ in (3.47), and after adding and subtracting appropriate terms, we find that

$$\begin{aligned} \beta_{\widehat{\mathbf{S}}} \|\omega - \widetilde{\omega}\|_{\mathrm{W}^{1,r}(\Omega)} &\leq \sup_{\theta \in \mathrm{W}^{1,s}(\Omega)\setminus\{0\}} \frac{[\mathscr{A}_{\boldsymbol{\sigma}}(\omega),\theta] - [\mathscr{A}_{\boldsymbol{\sigma}}(\widetilde{\omega}),\theta]}{\|\nabla\theta\|_{\mathbf{L}^s(\Omega)}} \\ &= \sup_{\theta \in \mathrm{W}^{1,s}(\Omega)\setminus\{0\}} \frac{[\mathscr{A}_{\widetilde{\boldsymbol{\sigma}}}(\widetilde{\omega}),\theta] - [\mathscr{A}_{\boldsymbol{\sigma}}(\widetilde{\omega}),\theta]}{\|\nabla\theta\|_{\mathbf{L}^s(\Omega)}} \\ &\leq d_3 \|\widetilde{\boldsymbol{\sigma}} - \boldsymbol{\sigma}\|_{\mathbb{L}^2(\Omega)} \|\nabla\widetilde{\omega}\|_{\mathbf{L}^{\frac{2r}{2-r}}(\Omega)}. \end{aligned} \tag{3.48}$$

Thus, the proof ends after combining the estimate (3.46) with (3.48), which leads to

$$\|\widetilde{\mathbf{S}}(\boldsymbol{\sigma}) - \widetilde{\mathbf{S}}(\widetilde{\boldsymbol{\sigma}})\|_{\mathrm{W}^{1,r}(\Omega)} := \|\omega - \widetilde{\omega}\|_{\mathrm{W}^{1,r}(\Omega)} \leq d_3 \beta_{\widehat{\mathbf{S}}}^{-1} C_{RE} \|J\|_{\mathrm{L}^2(\Omega)'} \|\widetilde{\boldsymbol{\sigma}} - \boldsymbol{\sigma}\|_{\mathbb{L}^2(\Omega)}. \qquad \square$$

Now, we are able to show the announced property of the operator $\mathbf{T}$.

LEMMA 3.16. *There exists a constant $C_{\mathbf{T}} > 0$ independent of λ_s such that*

$$\|\mathbf{T}(\omega_1) - \mathbf{T}(\omega_2)\|_{\mathrm{W}^{1,r}(\Omega)} \leq C_{\mathbf{T}} d_3 \beta \|J\|_{\mathrm{L}^2(\Omega)'} \|\omega_1 - \omega_2\|_{\mathrm{W}^{1,r}(\Omega)} \quad \forall\, \omega_1, \omega_2 \in \mathrm{W}^{1,r}_0(\Omega). \tag{3.49}$$

Proof. It suffices to recall from section 3.1 that $\mathbf{T}(\omega) = \widetilde{\mathbf{S}}(\mathbf{S}_2(\omega))\ \forall \omega \in \mathrm{W}^{1,r}_0(\Omega)$ and to apply Lemmas 3.14 and 3.15. $\square$

We can now establish the existence and uniqueness of a solution to (3.7a)–(3.7e), which follows straightforwardly from the Banach fixed-point theorem.

THEOREM 3.17. *Let $\mathbf{W}$ be as in (3.44) and r be such that $2d/(d+1) - \varepsilon < r < 2$ with $\varepsilon > 0$, and assume that $\beta_{\mathscr{A}}\phi < 1$ and that $C_{\mathbf{T}} d_3 \beta \|J\|_{\mathrm{L}^2(\Omega)'} < 1$. Then, there exists $\overline{C} > 0$, independent of λ_s, such that (3.7a)–(3.7e) has unique solution $(\boldsymbol{t}, \vec{\boldsymbol{\sigma}}, \vec{\boldsymbol{u}}, p, \omega) \in \mathbb{L}^2(\Omega) \times \mathbf{X} \times \mathbf{M} \times \mathrm{H}^1_\Sigma(\Omega) \times \mathrm{W}^{1,r}_0(\Omega)$ with $\omega \in \mathbf{W}$, satisfying*

$$\begin{aligned} &\|\boldsymbol{t}\|_{\mathbb{L}^2(\Omega)} + \|\vec{\boldsymbol{\sigma}}\|_{\mathbf{X}} + \|\vec{\boldsymbol{u}}\|_{\mathbf{M}} + \|p\|_{\mathrm{H}^1(\Omega)} + \|\omega\|_{\mathrm{W}^{1,r}(\Omega)} \\ &\qquad \leq \overline{C} \left(\|F\|_{\mathbf{M}'} + \|G\|_{\mathrm{H}^1_\Sigma(\Omega)'} + \|J\|_{\mathrm{W}^{1,r}_0(\Omega)'} \right). \end{aligned} \tag{3.50}$$

Proof. Thanks to Lemmas 3.13 and 3.16 and the assumption given in the statement of the present theorem, the existence of a unique solution is merely an application of the Banach fixed-point theorem. To prove (3.50), it suffices to apply the result (3.32) with $\widetilde{H}_\omega = H_\omega, \widetilde{F}_1 = \mathrm{O}, \widetilde{F} = F$, and $\widetilde{G} = G$; the estimate (3.43); the corresponding bound for $\|H_\omega\|_{\mathbb{L}^2(\Omega)'}$, and the fact that $\omega \in \mathbf{W}$. $\square$

4. Finite element method and solvability of the discrete problem. We now introduce and analyze the Galerkin scheme associated with (3.7a)–(3.7e). We consider generic finite dimensional subspaces

$$\begin{aligned} &\mathbb{H}^{\boldsymbol{t}}_h \subseteq \mathbb{L}^2(\Omega), \quad \mathbb{H}^{\boldsymbol{\sigma}}_h \subseteq \mathbb{H}_\Sigma(\mathbf{div},\Omega), \quad \mathrm{H}^{\widetilde{p}}_h(\Omega) \subseteq \mathrm{L}^2(\Omega), \quad \mathbf{H}^{\boldsymbol{u}}_h \subseteq \mathbf{L}^2(\Omega), \\ &\mathbb{H}^{\boldsymbol{\gamma}}_h(\Omega) \subseteq \mathbb{L}^2_{\mathrm{skew}}(\Omega), \quad \mathrm{H}^p_h \subseteq \mathrm{H}^1_\Sigma(\Omega), \quad \text{and} \quad \mathrm{H}^{\omega}_h \subseteq \mathrm{W}^{1,r}_0(\Omega), \end{aligned} \tag{4.1}$$

which will be specified later on. Then, we define

$$\vec{\boldsymbol{\sigma}}_h := (\boldsymbol{\sigma}_h, \widetilde{p}_h), \quad \vec{\boldsymbol{\tau}}_h := (\boldsymbol{\tau}_h, \widetilde{q}_h), \quad \vec{\boldsymbol{u}}_h := (\boldsymbol{u}_h, \boldsymbol{\gamma}_h), \quad \vec{\boldsymbol{v}}_h := (\boldsymbol{v}_h, \boldsymbol{\eta}_h),$$
$$\mathbf{X}_h := \mathbb{H}_h^{\boldsymbol{\sigma}} \times \mathrm{H}_h^{\widetilde{p}}, \quad \mathbf{M}_h := \mathbf{H}_h^{\boldsymbol{u}} \times \mathbb{H}_h^{\gamma},$$

and a Galerkin scheme for (3.7a)–(3.7e) reads as follows: Find $(\boldsymbol{t}_h, \vec{\boldsymbol{\sigma}}, \vec{\boldsymbol{u}}_h,\, p_h, \omega_h) \in \mathbb{H}_h^{\boldsymbol{t}} \times \mathbf{X}_h \times \mathbf{M}_h \times \mathrm{H}_h^p \times \mathrm{H}_h^{\omega}$ such that

$$[A(\boldsymbol{t}_h), \boldsymbol{r}_h] + [B^*(\vec{\boldsymbol{\sigma}}_h), \boldsymbol{r}_h] = [H_{\omega_h}, \boldsymbol{r}_h] \qquad \forall\, \boldsymbol{r}_h \in \mathbb{H}_h^{\boldsymbol{t}}, \tag{4.2a}$$

$$[B(\boldsymbol{t}_h), \vec{\boldsymbol{\tau}}_h] - [C(\vec{\boldsymbol{\sigma}}_h), \vec{\boldsymbol{\tau}}_h] + [B_1^*(\vec{\boldsymbol{u}}_h), \vec{\boldsymbol{\tau}}_h] + [B_2^*(p_h), \vec{\boldsymbol{\tau}}_h] = 0 \qquad \forall\, \vec{\boldsymbol{\tau}}_h \in \mathbf{X}_h, \tag{4.2b}$$

$$[B_1(\vec{\boldsymbol{\sigma}}_h), \vec{\boldsymbol{v}}_h] = [F, \vec{\boldsymbol{v}}_h] \qquad \forall\, \vec{\boldsymbol{v}}_h \in \mathbf{M}_h, \tag{4.2c}$$

$$[B_2(\vec{\boldsymbol{\sigma}}_h), q_h] - [D(p_h), q_h] = [G, q_h] \qquad \forall\, p_h \in \mathrm{H}_h^p, \tag{4.2d}$$

$$[\mathscr{A}_{\boldsymbol{\sigma}_h}(\omega_h), \theta_h] = [J, \theta_h] \qquad \forall\, \theta_h \in \mathrm{H}_h^{\omega}. \tag{4.2e}$$

In order to address the well-posedness of (4.2a)–(4.2e), we use again a fixed-point strategy. Let us define $\mathbf{S}_h : \mathrm{H}_h^{\omega} \to \mathbb{H}_h^{\boldsymbol{t}} \times \mathbf{X}_h \times \mathbf{M}_h \times \mathrm{H}_h^p$ as

$$\begin{aligned}\mathbf{S}_h(\omega_h) &:= (\mathbf{S}_{1,h}(\omega_h), (\mathbf{S}_{2,h}(\omega_h), \mathbf{S}_{3,h}(\omega_h)), (\mathbf{S}_{4,h}(\omega_h), \mathbf{S}_{5,h}(\omega_h)), \mathbf{S}_{6,h}(\omega_h)) \\ &= (\boldsymbol{t}_h, (\boldsymbol{\sigma}_h, \widetilde{p}_h), (\boldsymbol{u}_h, \boldsymbol{\gamma}_h), p_h) \in \mathbb{H}_h^{\boldsymbol{t}} \times \mathbf{X}_h \times \mathbf{M}_h \times \mathrm{H}_h^p,\end{aligned}$$

where $(\boldsymbol{t}_h, (\boldsymbol{\sigma}_h, \widetilde{p}_h), (\boldsymbol{u}_h, \boldsymbol{\gamma}_h), p_h)$ is the unique solution of (4.2a)–(4.2d) with ω_h given. In turn, let $\widetilde{\mathbf{S}}_h : \mathbb{H}_h^{\boldsymbol{\sigma}} \to \mathrm{H}_h^{\omega}$ be the operator defined by

$$\widetilde{\mathbf{S}}_h(\boldsymbol{\sigma}_h) := \omega_h \quad \forall\, \boldsymbol{\sigma}_h \in \mathbb{H}_h^{\boldsymbol{\sigma}},$$

where ω_h is the unique solution of (4.2e) with $\boldsymbol{\sigma}_h$ given. Finally, by introducing the operator $\mathbf{T}_h : \mathrm{H}_h^{\omega} \to \mathrm{H}_h^{\omega}$ as

$$\mathbf{T}_h(\omega_h) := \widetilde{\mathbf{S}}_h(\mathbf{S}_{2,h}(\omega_h)) \quad \forall\, \omega_h \in \mathrm{H}_h^{\omega},$$

we see that solving (4.2a)–(4.2e) is equivalent to seeking a fixed point of $\mathbf{T}_h$, that is, find $\omega_h \in \mathrm{H}_h^{\omega}$ such that

$$\mathbf{T}_h(\omega_h) = \omega_h. \tag{4.3}$$

4.1. Well definedness of the operator $\mathbf{T}_h$. Here we establish the solvability of (4.2a)–(4.2e) by studying the equivalent fixed-point problem (4.3). We begin by introducing some needed notations and preliminary results, as well as specific finite element subspaces satisfying (4.1).

Let us denote by $\mathcal{T}_h$ a regular partition of $\overline{\Omega}$ into triangles (or tetrahedra in three dimensions) K of diameter h_K, where $h := \max\{h_K : K \in \mathcal{T}_h\}$ is the meshsize. Given an integer $k \geq 0$, for each $K \in \mathcal{T}_h$ we let $\mathrm{P}_k(K)$ be the space of polynomial functions on K of degree $\leq k$ and define the local Raviart–Thomas space of order k as $\mathbf{RT}_k(K) := \mathbf{P}_k(K) \oplus \mathrm{P}_k(K)\,\boldsymbol{x}$, where $\mathbf{P}_k(K) = [\mathrm{P}_k(K)]^d$ and $\boldsymbol{x}$ is a generic vector in $\mathbb{R}^d$. Now, let b_K be the element bubble function defined as the unique polynomial in $\mathrm{P}_{d+1}(K)$ vanishing on ∂K with $\int_K b_K = 1$. Then, for each $K \in \mathcal{T}_h$ we consider the bubble space of order k, defined as

$$\mathbf{B}_k(K) := \begin{cases} \mathbf{curl}^{\mathrm{t}}(b_K \mathrm{P}_k(K)) & \text{in} \quad \mathbb{R}^2, \\ \nabla \times (b_K \mathbf{P}_k(K)) & \text{in} \quad \mathbb{R}^3. \end{cases}$$

On the other hand, we observe thanks to Lemma 3.5 that the ellipticity of $A:\mathbb{H}^{\boldsymbol{t}}_h\times\mathbb{H}^{\boldsymbol{t}}_h\to\mathbb{R}$ is satisfied for any finite dimensional subspace $\mathbb{H}^{\boldsymbol{t}}_h$ and with the same constant from (3.18). Therefore $\mathbb{H}^{\boldsymbol{t}}_h$ is chosen such that the discrete inf-sup condition for B holds. Moreover, thanks to the discrete analogue of B_1 (cf. (3.8c)), an inf-sup condition can be ensured by using the classical PEERS$_k$ elements introduced in [3], that is,

$$\begin{aligned}
\mathbb{H}^{\boldsymbol{\sigma}}_h &:= \left\{\boldsymbol{\tau}_h\in\mathbb{H}_\Sigma(\mathbf{div},\Omega):\quad \boldsymbol{\tau}_h|_K\in[\mathbf{RT}_k(K)]^d\oplus[\mathbf{B}_k(K)]^d\quad\forall\, K\in\mathcal{T}_h\right\},\\
\mathbf{H}^{\boldsymbol{u}}_h &:= \left\{\boldsymbol{v}_h\in\mathbf{L}^2(\Omega):\quad \boldsymbol{v}_h|_K\in\mathbf{P}_k(K)\quad\forall\, K\in\mathcal{T}_h\right\},\\
\mathbb{H}^{\gamma}_h &:= \left\{\boldsymbol{\eta}_h\in\mathbb{L}^2_{\mathrm{skew}}(\Omega):\quad \boldsymbol{\eta}_h\in\mathbf{C}(\overline{\Omega})\quad\text{and}\quad \boldsymbol{\eta}_h|_K\in\mathbb{P}_{k+1}(K)\quad\forall\, K\in\mathcal{T}_h\right\},
\end{aligned}\tag{4.4}$$

or by employing the well-known Arnold–Falk–Winther (AFW$_k$, [4]) family of order $k\geq 0$, that is,

$$\begin{aligned}
\mathbb{H}^{\boldsymbol{\sigma}}_h &:= \{\boldsymbol{\tau}_h\in\mathbb{H}_\Sigma(\mathbf{div},\Omega):\ \boldsymbol{\tau}_h|_K\in\mathbf{BDM}_{k+1}(K)\quad\forall\, K\in\mathcal{T}_h\},\\
\mathbf{H}^{\boldsymbol{u}}_h &:= \left\{\boldsymbol{v}_h\in\mathbf{L}^2(\Omega):\ \boldsymbol{v}_h|_K\in\mathbf{P}_k(K)\quad\forall\, K\in\mathcal{T}_h\right\},\\
\mathbb{H}^{\gamma}_h &:= \left\{\boldsymbol{\eta}_h\in\mathbb{L}^2_{\mathrm{skew}}(\Omega):\ \boldsymbol{\eta}_h|_K\in\mathbb{P}_k(K)\quad\forall\, K\in\mathcal{T}_h\right\}.
\end{aligned}\tag{4.5}$$

Also, we notice that the kernel of B_1 is given by

$$\mathbb{V}_h := \{\vec{\boldsymbol{\tau}}_h\in\mathbf{X}_h:\ [B_1(\vec{\boldsymbol{\tau}}_h),\vec{\boldsymbol{u}_h}]=0\quad\forall\,\vec{\boldsymbol{u}}_h\in\mathbf{M}_h\}.\tag{4.6}$$

Then, by using the definition given for $\mathbb{H}^{\boldsymbol{\sigma}}_h$, $\mathbf{H}^{\boldsymbol{u}}_h$, and $\mathbb{H}^{\gamma}_h$, (4.6) becomes $\mathbb{V}_h:=\mathbb{V}^{\boldsymbol{\sigma}}_h\times\mathrm{H}^p_h$, where

$$\mathbb{V}^{\boldsymbol{\sigma}}_h := \left\{\boldsymbol{\tau}_h\in\mathbb{H}^{\boldsymbol{\sigma}}_h:\ \mathbf{div}\,\boldsymbol{\tau}_h=0\quad\text{in}\quad\Omega\quad\text{and}\quad\int_\Omega\boldsymbol{\eta}_h:\boldsymbol{\tau}_h=0\quad\forall\,\boldsymbol{\eta}_h\in\mathbb{H}^{\gamma}_h\right\},\tag{4.7}$$

and therefore, if we use the finite elements (4.4), we can proceed as in [27, section 2.4] to extend the results given in [22] to the case $k\geq 1$ and define an appropriate space for $\mathbb{H}^{\boldsymbol{t}}_h$ as

$$\mathbb{H}^{\boldsymbol{t}}_h := \left\{\boldsymbol{r}_h\in\mathbb{L}^2(\Omega):\ \boldsymbol{r}_h|_K\in\mathbb{P}_k(K)\oplus[\mathbf{B}_k(K)]^d\oplus([\mathbf{B}_k(K)]^d)^{\mathrm{dev}}\quad\forall\, K\in\mathcal{T}_h\right\},\tag{4.8}$$

where $([\mathbf{B}_k(K)]^d)^{\mathrm{dev}}$ stands for the deviatoric part of tensor $[\mathbf{B}_k(K)]^d$. In turn, if (4.5) is employed, we simply take the part of the AFW$_k$ element that approximates $\boldsymbol{\sigma}$ without requiring $\mathbb{H}(\mathbf{div},\Omega)$-conformity, that is,

$$\mathbb{H}^{\boldsymbol{t}}_h := \left\{\boldsymbol{r}_h\in\mathbb{L}^2(\Omega):\ \boldsymbol{r}_h|_K\in\mathbf{BDM}_{k+1}(K)\quad\forall\, K\in\mathcal{T}_h\right\}.\tag{4.9}$$

Additionally, note that $\mathrm{H}^{\widetilde{p}}_h$ does not require any specific condition. It is therefore simply chosen as

$$\mathrm{H}^{\widetilde{p}}_h := \left\{\widetilde{q}_h\in\mathrm{L}^2(\Omega):\ \widetilde{q}_h|_K\in\mathrm{P}_k(K)\quad\forall\, K\in\mathcal{T}_h\right\}.\tag{4.10}$$

Finally, for pressure and solute concentration we consider Lagrange finite elements of degree $\leq k+1$, namely,

$$\mathrm{H}^p_h := \left\{q_h\in\mathrm{C}(\overline{\Omega})\cap\mathrm{H}^1_\Sigma(\Omega)\quad q_h|_K\in\mathrm{P}_{k+1}(K)\quad\forall\, K\in\mathcal{T}_h\right\},\tag{4.11a}$$

$$\mathrm{H}^{\omega}_h := \left\{\theta_h\in\mathrm{C}(\overline{\Omega})\cap\mathrm{W}^{1,s}_0(\Omega)\quad\theta_h|_K\in\mathrm{P}_{k+1}(K)\quad\forall\, K\in\mathcal{T}_h\right\},\tag{4.11b}$$

where $s>2$. Notice that, for each $h>0$, we have that $\mathrm{H}^{\omega}_h\subset\mathrm{W}^{1,s}_0(\Omega)\subset\mathrm{W}^{1,r}_0(\Omega)$.

We now require some preliminary results to establish the well-posedness of the operator $\mathbf{S}_h$.

LEMMA 4.1. *There exists $\hat{\beta}_{1_d} > 0$, independent of h, such that*

$$\sup_{\vec{\boldsymbol{\tau}}_h \in \mathbf{X}_h \setminus \{\mathbf{0}\}} \frac{[B_1(\vec{\boldsymbol{\tau}}_h), \vec{\boldsymbol{v}}_h]}{\|\vec{\boldsymbol{\tau}}_h\|_{\mathbf{X}}} \geq \hat{\beta}_{1_d} \|\vec{\boldsymbol{v}}_h\|_{\mathbf{M}} \quad \forall\, \vec{\boldsymbol{v}}_h \in \mathbf{M}_h. \tag{4.12}$$

LEMMA 4.2. *There exists $c_3 > 0$, independent of h, such that*

$$c_3 \|\boldsymbol{\tau}_h\|^2_{\mathbb{H}(\mathbf{div},\Omega)} \leq \|\boldsymbol{\tau}_{0,h}\|^2_{\mathbb{H}(\mathbf{div},\Omega)} \quad \forall\, \boldsymbol{\tau}_h \in \mathbb{H}^{\boldsymbol{\sigma}}_h.$$

Proof. The proof follows the same arguments from [22, Lemma 2.4] but now uses that $\boldsymbol{\tau}_h \boldsymbol{n} = \mathbf{0}\ \forall \boldsymbol{\tau}_h \in \mathbb{H}^{\boldsymbol{\sigma}}_h$. ∎

LEMMA 4.3. *There exists $\hat{\beta}_d > 0$, independent of h, such that*

$$\forall \sup_{\boldsymbol{r}_h \in \mathbb{H}^{\boldsymbol{t}}_h \setminus \{\mathbf{0}\}} \frac{[B(\boldsymbol{r}_h), \vec{\boldsymbol{\sigma}}_h]}{\|\boldsymbol{r}_h\|_{\mathbb{L}^2(\Omega)}} \geq \hat{\beta}_d \|\vec{\boldsymbol{\sigma}}_h\|_{\mathbf{X}} \quad \forall\, \vec{\boldsymbol{\sigma}}_h \in \mathbb{V}_h. \tag{4.13}$$

Proof. The proof follows applying Lemmas 3.1 and 4.2 and noticing that $\boldsymbol{\tau}_h^{\mathrm{dev}}$ and $(\widetilde{q}_h \mathbb{I} + \boldsymbol{\tau}_h) \in \mathbb{H}^{\boldsymbol{t}}_h$ for each $\vec{\boldsymbol{\tau}}_h \in \mathbb{V}_h$. We refer to [22, Lemma 2.5] for further details. ∎

Now, we are in a position to establish the well definedness of $\mathbf{T}_h$. First we guarantee that the discrete problems defined by $\mathbf{S}_h$ and $\widetilde{\mathbf{S}}_h$ are well-posed. In what follows, we show this result for $\mathbf{S}_h$, considering, as in the continuous case, generic functionals in (4.2a)–(4.2d), namely, $\widetilde{H}_{w_h}, \widetilde{F}_{1,h}, \widetilde{F}_h$, and $\widetilde{G}_h$ instead of H_{w_h}, O, F, and G, respectively.

LEMMA 4.4. *For each $\omega_h \in \mathrm{H}^{\omega}_h$ the problem* (4.2a)–(4.2d) *has a unique solution $(\boldsymbol{t}_h, \vec{\boldsymbol{\sigma}}_h, \vec{\boldsymbol{u}}_h, p_h) \in \mathbb{H}^{\boldsymbol{t}}_h \times \mathbf{X}_h \times \mathbf{M}_h \times \mathrm{H}^p_h$. Moreover, there exists $C_d > 0$ independent of h and λ_s such that*

$$\begin{aligned} \|\mathbf{S}_h(\omega_h)\| &= \|\boldsymbol{t}_h\|_{\mathbb{L}^2(\Omega)} + \|\vec{\boldsymbol{\sigma}}_h\|_{\mathbf{X}} + \|\vec{\boldsymbol{u}}_h\|_{\mathbf{M}} + \|p_h\|_{\mathrm{H}^1(\Omega)} \\ &\leq C_d \left(\|\widetilde{H}_{\omega_h}\|_{(\mathbb{H}^{\boldsymbol{t}}_h)'} + \|\widetilde{F}_{1,h}\|_{\mathbf{X}'} + \|\widetilde{F}_h\|_{\mathbf{M}'_h} + \|\widetilde{G}_h\|_{(\mathrm{H}^p_h)'} \right). \end{aligned} \tag{4.14}$$

Proof. The proof follows similarly to the proof for the continuous case. In fact, for the well-posedness of the discrete version of problem (3.35), we take advantage of the fact that for finite dimension, it suffices to prove that the homogeneous problem only has the trivial solution, which follows analogously to the proof of Lemma 3.7, whereas for the corresponding stability result (4.14), we proceed exactly as in Lemma 3.8. Therefore, by noticing that B satisfies the inf-sup condition (4.12), the proof follows the same steps as in Lemma 3.9 but now uses the arguments given by [25, Theorem 3.1]. ∎

Now, in order to establish the unique solvability of the nonlinear problem (4.2e), we recall the following result given in [8, Proposition 8.6.2].

LEMMA 4.5. *Let ϑ be an $n \times n$ matrix, satisfying the second and fourth conditions in* (3.6) *(taking ϑ instead of D). Then, there exist $h_0 > 0$ and $\varepsilon > 0$ such that, for each $0 < h \leq h_0$, there holds*

$$\widetilde{\beta}_{\mathscr{A}} \|\nabla \widetilde{\omega}_h\|_{\mathbf{L}^r(\Omega)} \leq \sup_{\theta_h \in \mathrm{H}^{\omega}_h \setminus \{\mathbf{0}\}} \frac{\int_\Omega \vartheta \nabla \widetilde{\omega}_h \cdot \nabla \theta_h}{\|\nabla \theta_h\|_{\mathbf{L}^s(\Omega)}} \qquad \forall\, \widetilde{\omega}_h \in \mathrm{H}^{\omega}_h, \tag{4.15}$$

where $2 - \varepsilon \leq r < 2$ and $\widetilde{\beta}_{\mathscr{A}}$ is a positive constant independent of h.

LEMMA 4.6. *Assume that* $\widetilde{\beta}_{\mathscr{A}}^{-1}\phi < 1$. *Then, for each* $\boldsymbol{\sigma}_h \in \mathbb{H}_h^{\boldsymbol{\sigma}}$, *there exist* $h_0 > 0$ *and* $\varepsilon > 0$ *such that, for each* $0 < h \leq h_0$ *and* $2 - \varepsilon \leq r < 2$, *the problem* (4.2e) *has a unique solution* $\omega_h := \widetilde{\mathbf{S}}_h(\boldsymbol{\sigma}_h) \in \mathrm{H}_h^{\omega}$. *Moreover, there holds*

$$\|\widetilde{\mathbf{S}}_h(\boldsymbol{\sigma}_h)\| := \|\omega_h\|_{\mathrm{W}^{1,r}(\Omega)} \leq \frac{\widetilde{\beta}_{\mathscr{A}}^{-1}}{1 - \widetilde{\beta}_{\mathscr{A}}^{-1}\phi}\|J\|_{(\mathrm{H}_h^{\omega})'}, \tag{4.16}$$

where $\widetilde{\beta}_{\mathscr{A}}^{-1}$ *is the discrete inf-sup constant given in* (4.15).

Proof. Lemma 4.5 helps us to apply the same steps as in the proof of Lemma 3.10 to obtain an equivalent discrete result to Lemma 3.10. The proof therefore follows simply as an application of that discrete result. ∎

4.2. Discrete solvability analysis. In this section we address the solvability of (4.3). We verify the hypotheses of the Brouwer fixed-point theorem to prove that (4.3) has at least one fixed point. Most of the details can be omitted since they follow straightforwardly by adapting the results given in section 3.3.

Let $\mathbf{W}_h := \{\omega_h \in \mathrm{H}_h^{\omega} : \ \|\omega_h\|_{\mathrm{W}^{1,r}(\Omega)} \leq \frac{\widetilde{\beta}_{\mathscr{A}}^{-1}}{1-\widetilde{\beta}_{\mathscr{A}}^{-1}\phi}\|J\|_{(\mathrm{H}_h^{\omega})'}\}$, be a compact and convex subset of H_h^{ω}. We now provide the discrete analogue of Lemma 3.13.

LEMMA 4.7. *Assume that* $\widetilde{\beta}_{\mathscr{A}}^{-1}\phi < 1$. *For the closed ball* $\mathbf{W}_h$, *it holds that* $\mathbf{T}_h(\mathbf{W}_h) \subseteq \mathbf{W}_h$.

On the other hand, it is not difficult to prove that for the discrete case the operator $\mathbf{S}_h$ satisfies the first bound in Lemma 3.14 with a constant $C_{\mathbf{S}_d} > 0$ instead of $C_{\mathbf{S}}$. With this goal in mind, we are now in a position to establish the following result.

LEMMA 4.8. *There exists a constant* $C_{\mathbf{T}_d} > 0$ *independent of* h *and* λ_s *such that*

$$\|\mathbf{T}_h(\omega_{1,h}) - \mathbf{T}_h(\omega_{2,h})\|_{\mathrm{W}^{1,r}(\Omega)} \leq C_{\mathbf{T}_d} d_3 \beta \|\nabla \mathbf{T}_h(\omega_{2,h})\|_{\mathbf{L}^{\frac{2r}{2-r}}(\Omega)} \|\omega_{1,h} - \omega_{2,h}\|_{\mathrm{W}^{1,r}(\Omega)} \quad \forall\, \omega_{1,h}, \omega_{2,h} \in \mathrm{H}_h^{\omega}. \tag{4.17}$$

Proof. Recalling from (4.3) the definition of $\mathbf{T}_h$, we notice, for each $\omega_{1,h}, \omega_{2,h} \in \mathrm{H}_h^{\omega}$, that

$$\begin{aligned} \|\mathbf{T}_h(\omega_{1,h}) - \mathbf{T}_h(\omega_{2,h})\|_{\mathrm{W}^{1,r}(\Omega)} &= \|\widetilde{\mathbf{S}}_h(\mathbf{S}_h(\omega_{1,h})) - \widetilde{\mathbf{S}}_h(\mathbf{S}_h(\omega_{2,h}))\|_{\mathrm{W}^{1,r}(\Omega)} \\ &\leq \frac{d_3}{\widetilde{\beta}_{\widetilde{\mathbf{S}}}} \|\nabla \widetilde{\mathbf{S}}_h(\mathbf{S}_h(\omega_{2,h}))\|_{\mathbf{L}^{\frac{2r}{2-r}}(\Omega)} \|\mathbf{S}_h(\omega_{2,h}) \\ &\quad - \mathbf{S}_h(\omega_{1,h})\|_{\mathbb{L}^2(\Omega)}, \end{aligned} \tag{4.18}$$

where, for the last inequality, we have applied the same arguments as in the proof of Lemma 3.15 but now for the discrete case. In this way, the bound in (4.17) follows from applying the Lipschitz continuity of the operator $\mathbf{S}_h$ and the definition of $\mathbf{T}_h$ to (4.18). ∎

We stress that [26, equation (4.14)] (where in the right-hand side, the term T_h should be read as ∇T_h) establishes a similar result as Lemma 4.8 (estimate (4.17) asserts the continuity of $\mathbf{T}_h$). However, here and also as in [26], the lack of control of one of the right-hand-side terms (we only know that it is bounded) does not allow us to conclude directly the Lipschitz continuity—and hence the contractivity—of this operator. For that reason, the main result of this section only yields existence of

a fixed point of $\mathbf{T}_h$, which follows as a consequence of Lemmas 4.7 and 4.8 and a straightforward application of the Brouwer fixed-point theorem.

We also remark that, although a precise estimate for the gradient of $\mathbf{T}_h(\omega_{2,h})$ in (4.17) is not obvious to obtain, we will provide numerical evidence that its norm is indeed bounded. See section 6, in particular, the last column of Tables 6.1 and 6.2.

THEOREM 4.9. *Let $\mathbf{W}_h$ be defined as at the beginning of this section, and assume that $\widetilde{\beta}_{\mathscr{A}}^{-1}\phi < 1$. Then, there exist $h_0 > 0$ and $\varepsilon > 0$ such that, for each $0 < h \leq h_0$ and $2 - \varepsilon \leq r < 2$, the coupled problem* (4.2a)–(4.2e) *has at least one solution $(\boldsymbol{t}_h, \vec{\boldsymbol{\sigma}}_h, \vec{\boldsymbol{u}}_h, p_h, \omega_h) \in \mathbb{H}_h^{\boldsymbol{t}} \times \mathbf{X}_h \times \mathbf{M}_h \times \mathrm{H}_h^p \times \mathrm{H}_h^\omega$ with $\omega_h \in \mathbf{W}_h$. Moreover, there exists $\overline{C}_d > 0$ independent of λ_s and h such that*

$$\begin{aligned}\|\boldsymbol{t}_h\|_{\mathbb{L}^2(\Omega)} + \|\vec{\boldsymbol{\sigma}}_h\|_{\mathbf{X}} + \|\vec{\boldsymbol{u}}_h\|_{\mathbf{M}} + \|p_h\|_{\mathrm{H}^1(\Omega)} + \|\omega_h\|_{\mathrm{W}^{1,r}(\Omega)} \\ \leq \overline{C}_d \left(\|F\|_{\mathbf{M}_h'} + \|G\|_{(\mathrm{H}_h^p)'} + \|J\|_{(\mathrm{H}_h^\omega)'} \right).\end{aligned}$$

Proof. We proceed similarly as in the continuous case. In fact, from (4.14) and (4.16), we get

$$\begin{aligned}\|\boldsymbol{t}_h\|_{\mathbb{L}^2(\Omega)} + \|\vec{\boldsymbol{\sigma}}_h\|_{\mathbf{X}} + \|\vec{\boldsymbol{u}}_h\|_{\mathbf{M}} + \|p_h\|_{\mathrm{H}^1(\Omega)} + \|\omega_h\|_{\mathrm{W}^{1,r}(\Omega)} \\ \leq \overline{C}_{1,d} \left(\|\widetilde{H}_{\omega_h}\|_{(\mathbb{H}_h^{\boldsymbol{t}})'} + \|\widetilde{F}_{1,h}\|_{\mathbf{X}_h'} + \|\widetilde{F}_h\|_{\mathbf{M}_h'} + \|\widetilde{G}_h\|_{(\mathrm{H}_h^p)'} + \|J\|_{(\mathrm{H}_h^\omega)'} \right).\end{aligned}$$

Then, the result follows by setting $\widetilde{H}_{\omega_h} = H_{\omega_h}$, $\widetilde{F}_{1,h} = \mathrm{O}$, $\widetilde{F}_h = F$, and $\widetilde{G}_h = G$, noticing that $\|H_{\omega_h}\|_{(\mathbb{H}_h^{\boldsymbol{t}})'} \leq C_H \|\omega_h\|_{\mathrm{W}^{1,r}(\Omega)}$, and applying the fact that $\omega_h \in \mathbf{W}_h$. ∎

5. Error analysis. In this section, we derive the optimal a priori error estimate. For this purpose, we first establish a Céa estimate formulated in the following theorem.

THEOREM 5.1. *Let $(\boldsymbol{t}, \vec{\boldsymbol{\sigma}}, \vec{\boldsymbol{u}}, p, \omega)$ and $(\boldsymbol{t}_h, \vec{\boldsymbol{\sigma}}_h, \vec{\boldsymbol{u}}_h, p_h, \omega_h)$ be the solutions of problems* (3.7a)–(3.7e) *and* (4.2a)–(4.2e)*, respectively, and assume that*

$$\hat{C}_{1,d} \left(C_H \beta + d_3 C_{RE} \|J\|_{\mathrm{L}^2(\Omega)'} \right) \leq \frac{1}{2}, \tag{5.1}$$

where $\hat{C}_{1,d}, C_H, \beta, d_3$, and C_{RE} are specified in (5.5)*,* (3.5)*,* (2.4b)*,* (3.6)*, and* (3.46)*, respectively. Then, there exists $C_{Céa} > 0$ such that*

(5.2)

$$\begin{aligned}\|\boldsymbol{t} - \boldsymbol{t}_h\|_{\mathbb{L}^2(\Omega)} + \|\vec{\boldsymbol{\sigma}} - \vec{\boldsymbol{\sigma}}_h\|_{\mathbf{X}} + \|\vec{\boldsymbol{u}} - \vec{\boldsymbol{u}}_h\|_{\mathbf{M}} + \|p - p_h\|_{\mathrm{H}^1(\Omega)} + \|\omega - \omega_h\|_{\mathrm{W}^{1,r}(\Omega)} \\ \leq C_{Céa} \left(\mathrm{dist}(\boldsymbol{t}, \mathbb{H}_h^{\boldsymbol{t}}) + \mathrm{dist}(\vec{\boldsymbol{\sigma}}, \mathbb{H}_h^{\vec{\boldsymbol{\sigma}}}) + \mathrm{dist}(\vec{\boldsymbol{u}}, \mathbf{H}_h^{\vec{\boldsymbol{u}}}) + \mathrm{dist}(p, \mathrm{H}_h^p) + \mathrm{dist}(\omega, \mathrm{H}_h^\omega) \right).\end{aligned}$$

Proof. For sake of notational convenience we define $\mathbf{e}_{\boldsymbol{t}} = \boldsymbol{t} - \boldsymbol{t}_h$, $\mathbf{e}_{\vec{\boldsymbol{\sigma}}} = \vec{\boldsymbol{\sigma}} - \vec{\boldsymbol{\sigma}}_h$, $\mathbf{e}_{\vec{\boldsymbol{u}}} = \vec{\boldsymbol{u}} - \vec{\boldsymbol{u}}_h$, $\mathrm{e}_p = p - p_h$, $\mathrm{e}_\omega = \omega - \omega_h$. As usual, for arbitrary $(\hat{\boldsymbol{r}}_h, \hat{\vec{\boldsymbol{\tau}}}_h, \hat{\vec{\boldsymbol{v}}}_h, \hat{q}_h, \hat{\theta}_h) \in \mathbb{H}_h^{\boldsymbol{t}} \times \mathbf{X}_h \times \mathbf{M}_h \times \mathrm{H}_h^p \times \mathrm{H}_h^\omega$, they are decomposed as

(5.3)

$$\mathbf{e}_{\boldsymbol{t}} = \boldsymbol{\xi}_{\boldsymbol{t}} + \boldsymbol{\chi}_{\boldsymbol{t}}, \quad \mathbf{e}_{\vec{\boldsymbol{\sigma}}} = \boldsymbol{\xi}_{\vec{\boldsymbol{\sigma}}} + \boldsymbol{\chi}_{\vec{\boldsymbol{\sigma}}}, \quad \mathbf{e}_{\vec{\boldsymbol{u}}} = \boldsymbol{\xi}_{\vec{\boldsymbol{u}}} + \boldsymbol{\chi}_{\vec{\boldsymbol{u}}}, \quad \mathrm{e}_p = \xi_p + \chi_p, \quad \text{and} \quad \mathrm{e}_\omega = \xi_\omega + \chi_\omega,$$

where

$$\boldsymbol{\xi}_{\boldsymbol{t}} := \boldsymbol{t} - \hat{\boldsymbol{r}}_h \in \mathbb{L}^2(\Omega),\ \boldsymbol{\chi}_{\boldsymbol{t}} := \hat{\boldsymbol{r}}_h - \boldsymbol{t}_h \in \mathbb{H}_h^{\boldsymbol{t}},\ \boldsymbol{\xi}_{\vec{\boldsymbol{\sigma}}} := \vec{\boldsymbol{\sigma}} - \hat{\vec{\boldsymbol{\tau}}}_h \in \mathbf{X},\ \boldsymbol{\chi}_{\vec{\boldsymbol{\sigma}}} := \hat{\vec{\boldsymbol{\tau}}}_h - \vec{\boldsymbol{\sigma}}_h \in \mathbf{X}_h,$$

$$\boldsymbol{\chi}_{\vec{\boldsymbol{u}}} := \hat{\vec{\boldsymbol{v}}}_h - \vec{\boldsymbol{u}}_h \in \mathbf{M}_h,$$

$$\xi_p := p - \hat{q}_h \in \mathrm{H}^1_\Sigma(\Omega),\ \chi_p := \hat{q}_h - p_h \in \mathrm{H}_h^p,\ \xi_\omega := \omega - \hat{\theta}_h \in \mathrm{W}_0^{1,r}(\Omega),\ \chi_\omega := \hat{\theta}_h - \omega_h \in \mathrm{H}_h^\omega.$$

Therefore, by subtracting (4.2a)–(4.2e) and (3.7a)–(3.7e), we easily get the classical Galerkin orthogonality, which together with the decompositions (5.3) implies that

$$
\begin{aligned}
[A(\boldsymbol{\chi}_{\boldsymbol{t}}),\boldsymbol{r}_h]+[B^*(\boldsymbol{\chi}_{\vec{\boldsymbol{\sigma}}}),\boldsymbol{r}_h]&=[H^h+H_{\omega-\omega_h},\boldsymbol{r}_h],\\
[B(\boldsymbol{\chi}_{\boldsymbol{t}}),\vec{\boldsymbol{\tau}}_h]-[C(\boldsymbol{\chi}_{\vec{\boldsymbol{\sigma}}}),\vec{\boldsymbol{\tau}}_h]+[B_1^*(\boldsymbol{\chi}_{\vec{\boldsymbol{u}}}),\vec{\boldsymbol{\tau}}_h]+[B_2^*(\chi_p),\vec{\boldsymbol{\tau}}_h]&=[\widetilde{F}_1^h,\vec{\boldsymbol{\tau}}_h],\\
[B_1(\boldsymbol{\chi}_{\vec{\boldsymbol{\sigma}}}),\vec{\boldsymbol{v}}_h]&=[F^h,\vec{\boldsymbol{v}}_h],\\
[B_2(\boldsymbol{\chi}_{\vec{\boldsymbol{\sigma}}}),q_h]-[D(\chi_p),q_h]&=[G^h,p_h],\\
[\mathscr{A}_{\boldsymbol{\sigma}_h}(\chi_\omega),\theta_h]&=[J^h+\mathscr{A}_{\boldsymbol{\sigma}_h}(\omega)-\mathscr{A}_{\boldsymbol{\sigma}}(\omega),\theta_h]
\end{aligned}
\tag{5.4}
$$

$\forall \boldsymbol{r}_h\in\mathbb{H}_h^{\boldsymbol{t}},\vec{\boldsymbol{\tau}}_h\in\mathbf{X}_h,\vec{\boldsymbol{v}}_h\in\mathbf{M}_h,p_h\in\mathrm{H}_h^p$, and $\theta_h\in\mathrm{H}_h^\omega$, and where

$$
\begin{aligned}
[H^h,\boldsymbol{r}_h]&:=-[A(\boldsymbol{\xi}_{\boldsymbol{t}}),\boldsymbol{r}_h]-[B^*(\boldsymbol{\xi}_{\vec{\boldsymbol{\sigma}}}),\boldsymbol{r}_h],\ [F^h,\vec{\boldsymbol{v}}]:=-[B_1(\boldsymbol{\xi}_{\vec{\boldsymbol{\sigma}}}),\vec{\boldsymbol{v}}_h],\\
[G^h,p_h]&:=-[B_2(\boldsymbol{\xi}_{\vec{\boldsymbol{\sigma}}}),q_h]+[D(\xi_p),q_h],\\
[J^h,\theta_h]&:=-[\mathscr{A}_{\boldsymbol{\sigma}_h}(\xi_p),\theta_h],\ [\widetilde{F}_1^h,\vec{\boldsymbol{\tau}}]:=-[B(\boldsymbol{\xi}_{\boldsymbol{t}}),\vec{\boldsymbol{\tau}}_h]+[C(\boldsymbol{\xi}_{\vec{\boldsymbol{\sigma}}}),\vec{\boldsymbol{\tau}}_h]\\
&\quad-[B_1^*(\boldsymbol{\xi}_{\vec{\boldsymbol{u}}}),\vec{\boldsymbol{\tau}}_h]-[B_2^*(\xi_p),\vec{\boldsymbol{\tau}}_h].
\end{aligned}
$$

Then, proceeding as in the proof of Theorem 4.9 but now for problem (5.4), we deduce that there exists $\hat{C}_{1,d}>0$, independent of λ_s and h, such that

$$
\begin{aligned}
&\|\boldsymbol{\chi}_{\boldsymbol{t}}\|_{\mathbb{L}^2(\Omega)}+\|\boldsymbol{\chi}_{\vec{\boldsymbol{\sigma}}}\|_{\mathbf{X}}+\|\boldsymbol{\chi}_{\vec{\boldsymbol{u}}}\|_{\mathbf{M}}+\|\chi_p\|_{\mathrm{H}^1(\Omega)}+\|\chi_\omega\|_{\mathrm{W}^{1,r}(\Omega)}\\
&\quad\le\hat{C}_{1,d}\Big(\|H^h+H_{\omega-\omega_h}\|_{(\mathbb{H}^{\boldsymbol{t}})'}+\|\widetilde{F}_1^h\|_{\mathbf{X}_h'}+\|F^h\|_{\mathbf{M}_h'}+\|G^h\|_{(\mathrm{H}_h^p)'}\\
&\qquad+\|J^h+\mathscr{A}_{\boldsymbol{\sigma}_h}(\omega)-\mathscr{A}_{\boldsymbol{\sigma}}(\omega)\|_{(\mathrm{H}_h^\omega)'}\Big).
\end{aligned}
\tag{5.5}
$$

In this way, we now proceed to bound the terms on the right-hand side of (5.5). We begin by noticing thanks to the continuity of the operators A and B^* and the definition of $H_{\omega-\omega_h}$ (cf. (3.8h)) that there holds

$$
\|H^h+H_{\omega-\omega_h}\|_{(\mathbb{H}^{\boldsymbol{t}})'}\le\hat{C}_1\left(\|\boldsymbol{\xi}_{\boldsymbol{t}}\|_{\mathbb{L}^2(\Omega)}+\|\boldsymbol{\xi}_{\vec{\boldsymbol{\sigma}}}\|_{\mathbf{X}}\right)+C_H\beta\|\mathrm{e}_\omega\|_{\mathrm{W}^{1,r}(\Omega)},
\tag{5.6}
$$

with $\hat{C}_1$ independent of λ_s and h. Proceeding in a similar way as before, it can be deduced that

$$
\begin{aligned}
&\|F^h\|_{\mathbf{M}_h'}\le\hat{C}_2\|\boldsymbol{\xi}_{\vec{\boldsymbol{\sigma}}}\|_{\mathbf{X}},\qquad\|G^h\|_{(\mathrm{H}_h^p)'}\le\hat{C}_3\left(\frac{\alpha}{\lambda_s}\|\boldsymbol{\xi}_{\vec{\boldsymbol{\sigma}}}\|_{\mathbf{X}}+\|\xi_p\|_{\mathrm{H}^1(\Omega)}\right),\\
&\|\widetilde{F}_1^h\|_{\mathbf{X}_h'}\le\hat{C}_4\left(\|\boldsymbol{\xi}_{\boldsymbol{t}}\|_{\mathbb{L}^2(\Omega)}+\frac{1}{\lambda_s}\|\boldsymbol{\xi}_{\vec{\boldsymbol{\sigma}}}\|_{\mathbf{X}}+\|\boldsymbol{\xi}_{\vec{\boldsymbol{u}}}\|_{\mathbf{M}}+\frac{\alpha}{\lambda_s}\|\xi_p\|_{\mathrm{H}^1(\Omega)}\right),
\end{aligned}
\tag{5.7}
$$

where $\hat{C}_2,\hat{C}_3,\hat{C}_4>0$ are independent of λ_s and h. On the other hand, in order to bound the last term on the right-hand side of (5.5), we proceed as in (3.48) to get

$$
\|\mathscr{A}_{\boldsymbol{\sigma}_h}(\omega)-\mathscr{A}_{\boldsymbol{\sigma}}(\omega)\|_{(\mathrm{H}_h^\omega)'}\le d_3\|\boldsymbol{\sigma}-\boldsymbol{\sigma}_h\|_{\mathbb{L}^2(\Omega)}\|\nabla\omega\|_{\mathbf{L}^{\frac{2r}{2-r}}(\Omega)},
$$

and then, from the latter, we conclude that

$$
\|J^h+\mathscr{A}_{\boldsymbol{\sigma}_h}(\omega)-\mathscr{A}_{\boldsymbol{\sigma}}(\omega)\|_{(\mathrm{H}_h^\omega)'}\le\hat{C}_5\|\xi_\omega\|_{\mathrm{W}^{1,r}(\Omega)}+d_3\|\mathbf{e}_{\vec{\boldsymbol{\sigma}}}\|_{\mathbf{X}}\|\nabla\omega\|_{\mathbf{L}^{\frac{2r}{2-r}}(\Omega)},
\tag{5.8}
$$

with $\hat{C}_5$ independent of λ_s and h. Therefore, from (5.6), (5.7), and (5.8), we obtain that there exists $\hat{C}_{2,d}>0$ independent of λ_s and h such that

$$
\begin{aligned}
&\|\boldsymbol{\chi}_{\boldsymbol{t}}\|_{\mathbb{L}^2(\Omega)}+\|\boldsymbol{\chi}_{\vec{\boldsymbol{\sigma}}}\|_{\mathbf{X}}+\|\boldsymbol{\chi}_{\vec{\boldsymbol{u}}}\|_{\mathbf{M}}+\|\chi_p\|_{\mathrm{H}^1(\Omega)}+\|\chi_\omega\|_{\mathrm{W}^{1,r}(\Omega)}\\
&\quad\le\hat{C}_{2,d}\left(\|\boldsymbol{\xi}_{\boldsymbol{t}}\|_{\mathbb{L}^2(\Omega)}+\left(1+\frac{1}{\lambda_s}+\frac{\alpha}{\lambda_s}\right)\|\boldsymbol{\xi}_{\vec{\boldsymbol{\sigma}}}\|_{\mathbf{X}}+\|\boldsymbol{\xi}_{\vec{\boldsymbol{u}}}\|_{\mathbf{M}}\right.\\
&\qquad\left.+\left(1+\frac{\alpha}{\lambda_s}\right)\|\xi_p\|_{\mathrm{H}^1(\Omega)}+\|\xi_\omega\|_{\mathrm{W}^{1,r}(\Omega)}\right)\\
&\quad+d_3\hat{C}_{1,d}C_{RE}\|J\|_{\mathrm{L}^2(\Omega)'}\|\mathbf{e}_{\vec{\boldsymbol{\sigma}}}\|_{\mathbf{X}}+\hat{C}_{1,d}\beta\|\mathrm{e}_\omega\|_{\mathrm{W}^{1,r}(\Omega)},
\end{aligned}
\tag{5.9}
$$

where we have applied the regularity estimate given by (3.46) and $(1+\frac{1}{\lambda_s}+\frac{\alpha}{\lambda_s})$ and $(1+\frac{\alpha}{\lambda_s})$ can be seen as constants independent of λ_s if $\lambda_s \to \infty$. In this way, the desired result follows simply by the triangle inequality in (5.3), the estimation (5.9), and assumption (5.1). ∎

The main result of this section is given by the following lemma.

THEOREM 5.2. *In addition to the hypotheses of Theorems* 3.17*,* 4.9*, and* 5.1*, assume that there exist* $t > 0$ *and* $l > 1/2$ *such that* $\boldsymbol{\sigma} \in \mathbb{H}^t(\Omega)$*,* $\mathbf{div}\,\boldsymbol{\sigma} \in \mathbf{H}^t(\Omega)$*,* $\boldsymbol{u} \in \mathbf{H}^t(\Omega)$*,* $\boldsymbol{\gamma} \in \mathbb{H}^t(\Omega)$*,* $\widetilde{p} \in \mathrm{H}^t(\Omega)$*,* $p \in \mathrm{H}^{1+t}(\Omega)$*,* $\omega \in \mathrm{W}^{1+t,r}(\Omega)$*, and* $\boldsymbol{t} \in \mathbb{H}^l(\Omega)$*. Then, there exist* $\widetilde{C}_1, \widetilde{C}_2 > 0$*, independent of* h*, such that, with the finite element subspaces defined by* (4.5)*,* (4.9)*,* (4.10)*,* (4.11a)*, and* (4.11b)*, there holds*

(5.10)

$$\begin{aligned}\|\boldsymbol{t}-\boldsymbol{t}_h\|_{\mathbb{L}^2(\Omega)} + \|\vec{\boldsymbol{\sigma}}-\vec{\boldsymbol{\sigma}}_h\|_{\mathbf{X}} + \|\vec{\boldsymbol{u}}-\vec{\boldsymbol{u}}_h\|_{\mathbf{M}} + \|p-p_h\|_{\mathrm{H}^1(\Omega)} + \|\omega-\omega_h\|_{\mathrm{W}^{1,r}(\Omega)}\\ \leq \widetilde{C}_1 h^{\min\{t,k+1\}} \Big\{ \|\boldsymbol{\sigma}\|_{\mathbb{H}^t(\Omega)} + \|\mathbf{div}\,\boldsymbol{\sigma}\|_{\mathbf{H}^t(\Omega)} + \|\boldsymbol{u}\|_{\mathbf{H}^t(\Omega)} + \|\boldsymbol{\gamma}\|_{\mathbb{H}^t(\Omega)} + \|\widetilde{p}\|_{\mathrm{H}^t(\Omega)}\\ + \|p\|_{\mathrm{H}^{1+t}(\Omega)} + \|\omega\|_{\mathrm{W}^{1+t,r}(\Omega)} \Big\} + \widetilde{C}_2 h^{\min\{l,k+1\}} \|\boldsymbol{t}\|_{\mathbb{H}^l(\Omega)}.\end{aligned}$$

Proof. The proof follows as a combination of Céa estimate (5.2), the smallness assumption, and the approximation properties of the spaces (4.5), (4.9), (4.10), (4.11a), and (4.11b). In particular, for the concentration approximability we use a quasi-interpolator $\mathcal{I}^{\mathrm{av}}_{h0} : \mathrm{W}^{1+t,r} \to \mathrm{H}^{\omega}_h$ with the local property (see [19, Theorem 6.4])

$$|\omega - \mathcal{I}^{\mathrm{av}}_{h0}\omega|_{\mathrm{W}^{1,r}(K)} \leq C h_K^t |\omega|_{\mathrm{W}^{1+t,r}(K)}$$

with $t \in [0, k+1]$ (we recall that in the notation of section 4.1, the discrete space H^{ω}_h is conformed by P_{k+1} elements). ∎

Remark 5.3. Similar results are obtained when (4.4) and (4.8) are employed instead of (4.5) and (4.9), respectively. For the lowest-order case, we notice from the classical approximation properties of the finite element subspaces that it suffices to consider $l > 0$, and therefore, the second to last term on the right-hand side of (5.10) should be changed to $\widetilde{C}_1 h^{\min\{t,k+1\}} \sum_{K\in\mathcal{T}_h} \|\boldsymbol{t}\|_{\mathbb{H}^t(K)}$ (see [22, Theorem 3.2]), whereas the other terms remain unchanged. Even if approximation results for (4.8) in the high-order case do not seem to be available in the literature, the numerical results in the next section demonstrate an asymptotic $\mathcal{O}(h^{k+1})$ convergence (see Table 6.1).

6. Numerical tests.

6.1. Example 1: Convergence against manufactured solutions. The accuracy of the discretization is verified through two convergence tests using manufactured solutions and implemented using the FEniCS library [40]. The model parameters are simply taken as $\mu_s = \lambda_s = 1 = c_0 = \kappa = \alpha = \ell = \rho_f = \rho_s = \mu_f = \beta = 1$, and $\phi = 0.5$, and $\boldsymbol{g} = \mathbf{0}$. Variations (of several orders of magnitude) in λ_s, α, μ_f and the pair (κ, c_0) will be also considered to study the robustness of the formulation with respect to these parameters. The stress-altered diffusion is (2.3) with $D_0 = 0.01$ and $\eta = 0.01$. We use the following closed-form smooth solutions to (2.4),

$$\omega = e^{x_1} + \cos(\pi x_1)\cos(\pi x_2),\ \boldsymbol{u} = \frac{1}{10}\begin{pmatrix} -\cos(x_1)\sin(x_2) + \frac{x_1^2}{\lambda_s} \\ \sin(x_1)\cos(x_2) + \frac{x_2^2}{\lambda_s} \end{pmatrix},$$
$$p = \sin(\pi x_1)\sin(\pi x_2),\ \widetilde{p} = \alpha p - \lambda_s \mathrm{div}\,\boldsymbol{u},$$

TABLE 6.1

Verification of convergence for the method with PEERS$_k$ and enriched piecewise polynomials with degrees $k=0$ and $k=1$ and using unity parameters. Errors and convergence rates are tabulated for strain, stress, total pressure, displacement, rotation Lagrange multiplier, fluid pressure, and tracer concentration (measured in the $\mathrm{W}^{1,r}$-norm with $r=\frac{3}{2}$). The last column shows the norm of the gradient of the fixed-point operator applied to the discrete tracer solution (6.1). *The asterisks in all tables indicate that no rates are computed at the first refinement level.*

DoF	$e_0(\boldsymbol{t})$	Rate	$e_{\mathbf{div}}(\boldsymbol{\sigma})$	Rate	$e_1(\tilde{p})$	Rate	$e_0(\boldsymbol{u})$	Rate	$e_0(\boldsymbol{\gamma})$	Rate	$e_1(p)$	Rate	$e_{1,r}(\omega)$	Rate	$\hat{\varphi}_h$
Scheme with $k=0$															
148	1.8e-01	*	1.2e+00	*	2.8e-01	*	2.6e-02	*	3.2e-01	*	1.1e+0	*	1.7e+0	*	2.35
540	7.8e-02	1.19	6.2e-01	0.99	1.4e-01	1.00	8.6e-03	1.59	9.6e-02	1.73	7.4e-01	0.62	8.8e-01	0.94	2.46
2068	3.7e-02	1.08	3.1e-01	1.00	6.8e-02	1.07	3.9e-03	1.15	3.7e-02	1.36	4.1e-01	0.85	4.3e-01	1.03	2.44
8100	1.8e-02	1.05	1.6e-01	1.00	3.3e-02	1.03	1.9e-03	1.04	1.4e-02	1.43	2.1e-01	0.95	2.1e-01	1.03	2.44
32068	8.7e-03	1.03	7.8e-02	1.00	1.6e-02	1.01	9.4e-04	1.01	5.0e-03	1.48	1.1e-01	0.98	1.0e-01	1.02	2.44
127620	4.3e-03	1.02	3.9e-02	1.00	8.2e-03	1.00	4.7e-04	1.00	1.8e-03	1.50	5.4e-02	1.00	5.1e-02	1.01	2.44
509188	2.5e-03	1.01	1.9e-02	1.00	4.1e-03	1.00	2.3e-04	1.00	1.5e-03	1.20	2.7e-02	1.00	2.6e-02	1.00	2.44
Scheme with $k=1$															
436	1.3e-02	*	2.3e-01	*	7.7e-02	*	1.8e-03	*	6.9e-03	*	3.8e-01	*	4.8e-01	*	2.49
1652	4.6e-03	1.51	5.8e-02	1.97	2.0e-02	1.95	4.4e-04	2.02	2.4e-03	1.35	1.2e-01	1.70	1.3e-01	1.88	2.44
6436	1.3e-03	1.76	1.5e-02	1.99	5.0e-03	1.99	1.0e-04	2.07	8.7e-04	1.44	3.2e-02	1.88	3.3e-02	1.96	2.44
25412	3.6e-04	1.91	3.7e-03	2.00	1.2e-03	2.00	2.5e-05	2.04	2.5e-04	1.78	8.2e-03	1.95	8.4e-03	1.99	2.44
100996	9.2e-05	1.96	9.2e-04	2.00	3.1e-04	2.00	6.3e-06	2.01	6.7e-05	1.91	2.1e-03	1.98	2.1e-03	2.00	2.44
402692	2.3e-05	1.98	2.3e-04	2.00	7.8e-05	2.00	1.6e-06	2.00	1.7e-05	1.96	5.2e-04	1.99	5.3e-04	2.00	2.44
1608196	5.9e-06	1.99	5.7e-05	2.00	1.9e-05	2.00	3.9e-07	2.00	4.4e-06	1.98	1.3e-04	2.00	1.3e-04	2.00	2.44

which are used to produce nonhomogeneous forcing and source terms. For the sake of simplicity only one type of boundary conditions is considered, i.e., $\partial\Omega=\Gamma$. The remaining boundary conditions in (2.4g) (for displacement and fluid flux) are imposed naturally. This also implies that the stress is not uniquely defined, and we constraint its trace, using a real Lagrange multiplier. We generate seven successively refined meshes (congruent right-angled triangular partitions) for the domain $\Omega=(0,1)^2$ and calculate errors between approximate and exact solutions $e(\cdot)$ (measured in H^1-norm for fluid pressure; in $\mathrm{W}^{1,r}$-norm for the tracer; in the tensor $\mathbf{H}(\mathrm{div})$-norm for stress; and in the tensorial, vectorial, and scalar L^2-norm for strain, rotation, displacement, and total pressure). We take the Sobolev exponent $r=\frac{3}{2}$. The mixed finite element methods are defined by the PEERS$_k$ and enriched piecewise polynomial spaces specified in (4.4), (4.8), and (4.11a).

Table 6.1 shows such error decay for polynomial orders $k=0$ and $k=1$, and we can clearly observe a convergence of $O(h^{k+1})$ for all field variables in their natural norms, which is consistent with the theoretical error bounds. Table 6.2 shows the error history associated with the extension to three dimensions, using the exact solutions

$$\omega=\cos(\pi x_1)\cos(\pi x_2)\cos(\pi x_3),\ \boldsymbol{u}=\frac{1}{10}\begin{pmatrix}\sin(x_1)\cos(x_2)\cos(x_3)+\frac{x_1^2}{\lambda_s}\\ -2\cos(x_1)\sin(x_2)\cos(x_3)+\frac{x_2^2}{\lambda_s}\\ \cos(x_1)\cos(x_2)\sin(x_3)+\frac{x_3^2}{\lambda_s}\end{pmatrix},$$
$$p=\sin(\pi x_1)\sin(\pi x_2)\sin(\pi x_3),$$

and $\widetilde{p}=\alpha p-\lambda_s\mathrm{div}\boldsymbol{u}$, on $\Omega=(0,1)^3$, with the same unit parameters, and focusing on the lowest-order scheme. Optimal, first-order convergence is also achieved in this case. For completeness, we also verify the error decay of the scheme resulting from using AFW$_k$ elements (4.5) and (4.9), which also delivers optimal convergence.

TABLE 6.2

Verification of space convergence in three dimensions with polynomial degree $k = 0$ and using unity parameters. Errors history for strain, stress, total pressure, displacement, rotation Lagrange multiplier, fluid pressure, and tracer concentration (measured in the $\mathrm{W}^{1,r}$-norm with $r = \frac{3}{2}$). The last column shows the norm of the gradient of the fixed-point operator applied to the discrete tracer solution (6.1).

DoF	$e_0(\boldsymbol{t})$	Rate	$e_{\mathbf{div}}(\boldsymbol{\sigma})$	Rate	$e_1(\tilde{p})$	Rate	$e_0(\boldsymbol{u})$	Rate	$e_0(\boldsymbol{\gamma})$	Rate	$e_1(p)$	Rate	$e_{1,r}(\omega)$	Rate	$\hat{\varphi}_h$
Scheme with PEERS_k and enriched piecewise polynomials															
1984	1.7e-01	*	1.5e+0	*	2.0e-01	*	2.0e-02	*	1.4e-01	*	1.4e+0	*	1.6e+0	*	2.29
6477	9.8e-02	0.72	1.0e+0	0.87	1.5e-01	0.74	1.3e-02	0.99	8.3e-02	1.29	9.4e-01	0.63	1.2e+0	0.73	2.27
29281	6.4e-02	0.83	6.4e-01	0.95	8.9e-02	0.98	7.7e-03	1.08	2.7e-02	2.16	6.7e-01	0.76	7.7e-01	0.90	2.21
168297	3.5e-02	0.92	3.6e-01	0.99	4.7e-02	1.09	4.1e-03	1.07	1.0e-02	1.71	4.1e-01	0.84	4.3e-01	0.98	2.20
1125049	2.1e-02	0.95	1.9e-01	1.00	2.4e-02	1.06	2.1e-03	1.04	3.7e-03	1.59	2.2e-01	0.96	2.3e-01	1.00	2.19
8194137	1.2e-02	0.96	9.6e-02	1.01	1.3e-02	1.02	1.1e-03	1.00	1.6e-03	1.49	1.2e-01	0.97	1.2e-01	0.98	2.19
Scheme with AFW_k elements															
2551	7.1e-02	*	1.4e+0	*	1.9e-01	*	1.9e-02	*	3.8e-02	*	1.3e+0	*	1.6e+0	*	2.29
8067	4.3e-02	1.24	1.0e+0	0.90	1.4e-01	0.78	1.2e-02	1.04	2.2e-02	1.38	9.4e-01	0.59	1.2e+0	0.74	2.27
35383	2.3e-02	1.23	6.1e-01	0.96	8.5e-02	0.99	7.4e-03	1.02	1.1e-02	1.35	6.7e-01	0.66	7.7e-01	0.91	2.21
198831	1.0e-02	1.34	3.4e-01	0.99	4.6e-02	1.06	4.0e-03	1.02	5.0e-03	1.32	4.1e-01	0.84	4.3e-01	0.98	2.20
1310431	4.6e-03	1.31	1.8e-01	1.00	2.4e-02	1.03	2.1e-03	1.01	2.3e-03	1.22	2.3e-01	0.94	2.3e-01	0.99	2.19

One of the key components of our analysis is the use of a fixed-point argument for the solution of the problem. In order to illustrate numerically the Lipschitz continuity of the discrete fixed-point operator $\mathbf{T}_h$ (cf. Lemma 4.8), we have tabulated the $\mathbf{L}^{\frac{2r}{2-r}}(\Omega)$-norm of its gradient

$$\hat{\varphi}_h := \|\nabla \mathbf{T}_h(\omega_h)\|_{\mathbf{L}^{\frac{2r}{2-r}}(\Omega)}. \tag{6.1}$$

These values converge to a constant with a value of 2.44 in Table 6.1 and 2.19 in Table 6.2. This indicates that $\hat{\varphi}_h$ remains bounded.

Figure 6.1 illustrates the robustness with respect to large variations in physical parameters including nearly incompressible materials (taking $\lambda_s = 10^8$), for low permeability and low storativity (with $\kappa = 10^{-12}$ and $c_0 = 10^{-6}$), for weak Biot–Willis coupling ($\alpha = 10^{-6}$), and with small fluid viscosity (with $\mu_f = 10^{-4}$). Analogous results (not shown here) were obtained for different values of porosity. For all these tests (both 2D and 3D), on average, four Newton–Raphson iterations were required to reach convergence across all mesh refinements.

6.2. Example 2: Testing the effect of stress-altered diffusion. In this test we compare the filtration effects on models using different degrees of stress-modified diffusion where the diffusion due to stress is lower than the constant base-line diffusion. This simple test emphasizes the significance of anisotropy and heterogeneity in the transport of tracer, and it is more illustrative to consider the time-dependent case (adding a time derivative of the first two terms in the second equation of (2.1) and of the first term in (2.2), which we discretize using the backward Euler method with a constant time step. For this we employ a slab of tissue of size 1 mm^2, and the model parameters are as follows (see, e.g., [10, 31, 50]):

$$E = 800\,\mathrm{Pa},\ \nu = 0.495,\ c_0 = 2 \times 10^{-8},\ \kappa = 10^{-8}\,\mathrm{mm}^2,\ \alpha = 1,\ \ell = 0,$$
$$\rho_s = 10^{-3}\,\mathrm{mg/mm}^3,$$

$$\mu_f = 0.7\,\mathrm{Pa\ s},\ \beta = 0.45,\ \phi = 0.2,\ D_0 = 5.3 \times 10^{-5}\mathrm{mm}^2/\mathrm{s},$$

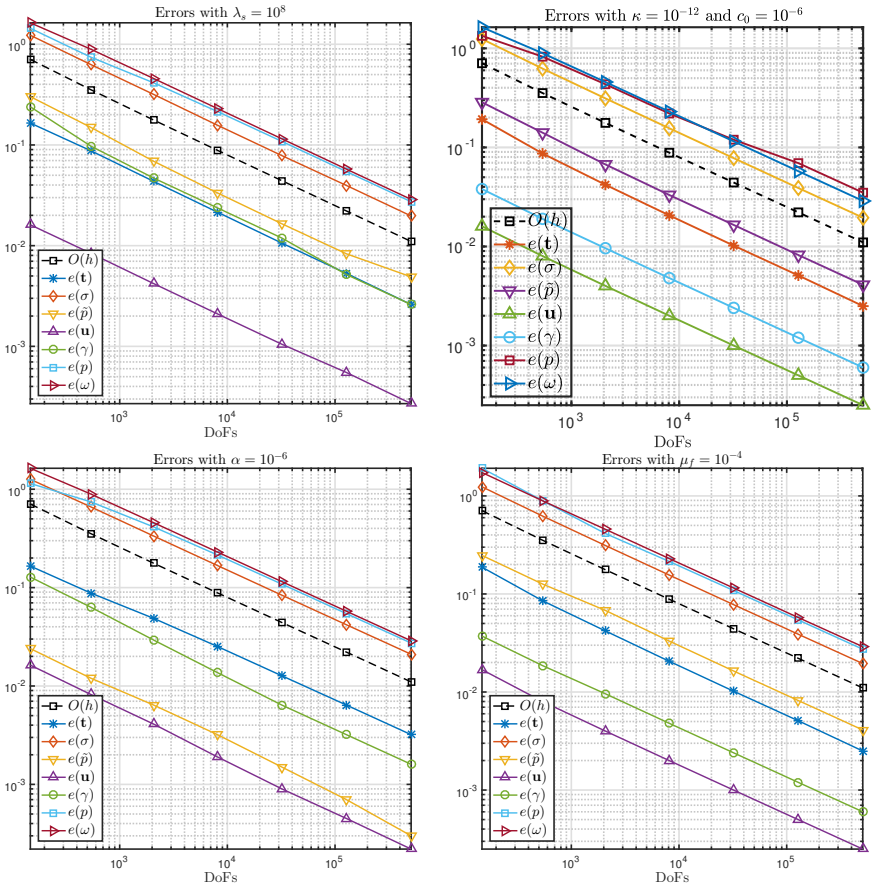

FIG. 6.1. *Verification of space convergence and robustness with respect to changes in model parameters* $\lambda_s, (\kappa, c_0), \alpha, \mu_f$.

where D_0 is made sufficiently large to compare with stress-hindered effects. On the top of the slab we impose a traction $\boldsymbol{\sigma n} = -\alpha p_{\text{top}} \boldsymbol{n}$ with $p_{\text{in}} = 0.5 \operatorname{atan}(t/10)$ mmHg/mm, on the bottom we clamp the tissue $\boldsymbol{u} = \mathbf{0}$, and on the vertical walls we set zero traction. The fluid pressure p_{in} is prescribed on the top segment and set to $p_0 = 9$ mmHg/mm on the vertical walls, whereas we set zero normal flux on the bottom. The tracer concentration $\omega_{\text{in}} = 1$ mmol is fixed on the top, and zero diffusive flux is considered elsewhere on the boundary. A coarse mesh with 16384 triangular elements is employed, and the time step is $\Delta t = 50$ s.

Three main scenarios are considered: (a) pure reaction-diffusion of the tracer with D_0, (b) adding the effect of isotropic stress-assisted diffusion according to

$$D(\boldsymbol{\sigma}) = D_0 \mathbb{I} + D_0 \exp(-\eta_0 \operatorname{tr} \boldsymbol{\sigma}) \mathbb{I} \tag{6.2}$$

with $\eta_0 = 5 \times 10^{-5}$, and (c) modifying the functional form of the apparent diffusion to

$$\tilde{D}(\boldsymbol{\sigma}) = \eta_0 D_0 \mathbb{I} - \eta_1 D_0 \boldsymbol{\sigma} + \eta_2 D_0 \boldsymbol{\sigma}^2 \tag{6.3}$$

with $\eta_1 = 0.02$ and $\eta_2 = 10^{-5}$. Figure 6.2 shows the results from these tests. The first row illustrates how with pure diffusion (without stress-hinderance) the tracer

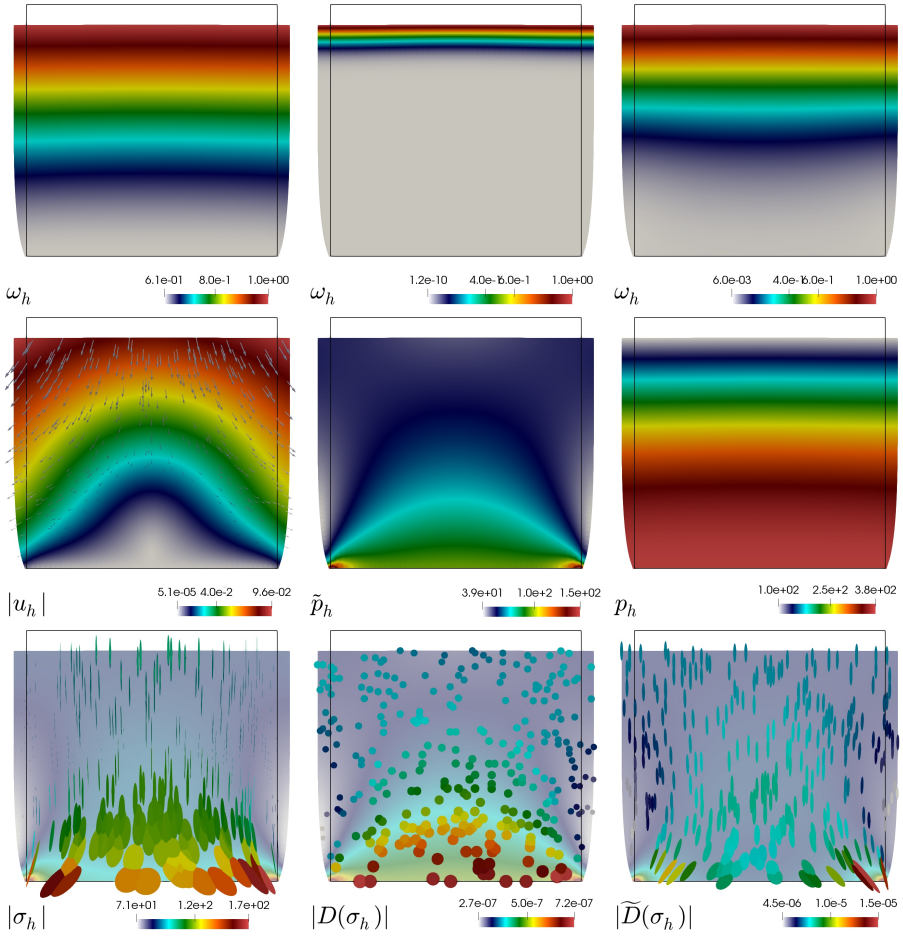

FIG. 6.2. *Example* 2. *Stress-altered diffusion. Top: Filtration of the CSF tracer into the slab of tissue for pure reaction-diffusion (left), stress-hindered diffusion according to* (6.2) *(center), and the anisotropic form* (6.3) *(right). Middle row: Approximate displacement (left), total pressure (center), and fluid pressure (right). Bottom: Tensor glyph representation on the deformed configuration, of the total Cauchy stress (left), the isotropic diffusion (center), and anisotropic one (right). All snapshots are taken at time* $t = 1800$ *s.*

penetrates faster than in the cases with stress-dependent diffusion (this is shown at $t = 1800$ s). The deformation of the parenchymal slab using case (c) is shown in the second row, where we can observe a localization of total pressure accumulation near the bottom corners of the domain. The bottom row indicates the degree of anisotropy of the total poroelastic stress and of the stress-altered diffusivity tensors according to (6.2) and (6.3), also at $t = 1800$ s. In case (c), apart from a slower diffusion than in case (a), a slight deviation from plane solute transport is seen (in the top-right panel of the figure), explained by the anisotropy differences exhibited in the bottom row of the figure.

6.3. Example 3: Stress-hindered diffusion and transport in the brain. Next we perform two application tests investigating the filtration properties of parenchymal brain tissue and the evolution of tracer concentration in its sleeping versus awake

state. Transport in the brain has been reported to occur 5%–24% faster than diffusion [52], suggesting diffusion is the dominant mechanism of transport. We therefore neglect convection to assess whether stress-dependent diffusion may explain the discrepancy between observations and Fickian diffusion simulations. In the first example, we create a 2D slab (1 mm deep, 1 μm wide) of a mouse brain, and simulated tracer enrichment from the cortical surface into the cortex. The diffusion coefficient was here assumed to take the form

$$D(\boldsymbol{\sigma}) = D_0\mathbb{I} - D_0 \exp(-\eta|\mathrm{tr}(\boldsymbol{\sigma})|)\mathbb{I}. \tag{6.4}$$

Boundary conditions for the first test case (in two dimensions) assume the form

$$\begin{aligned} \omega = 1, \quad p = p_0, \quad \boldsymbol{\sigma}\boldsymbol{n} &= -p_0 \arctan(t/50)\boldsymbol{n} && \text{on cortex (top)},\\ D(\boldsymbol{\sigma})\nabla\omega\cdot\boldsymbol{n} = \kappa\nabla p\cdot\boldsymbol{n} &= 0 && \text{on sides and bottom},\\ \boldsymbol{\sigma}\boldsymbol{n} &= \boldsymbol{0} && \text{on sides},\\ \boldsymbol{u} &= \boldsymbol{0} && \text{on bottom}, \end{aligned}$$

and the initial condition is $\omega = 0$ everywhere. The depth (1 mm) was assumed to cover the entire width of the mouse cortex. Over time we measured the concentration (100 μm into the tissue) similarly to the results reported by [54]. In the awake state, the porosity was set to $\phi = 0.14$, while in the awake state we used $\phi = 0.23$ [54]. We assumed that the known change in volume fraction was associated with a similar change in the width of the cerebral cortex, which is known to change during sleep [16]. Simulating the (compressed) awake state, we therefore added a force $\boldsymbol{\sigma}\boldsymbol{n} = -p_0 \arctan(\frac{t}{50s})\boldsymbol{n}$, where $p_0 = 0.5$ mmHg to the top of the domain, while the bottom was fixed. The arctan function was used to ensure a smooth loading. In the sleeping state, no forces were applied, and tracers were thus allowed to diffuse freely according to the base diffusion D_0. In both cases the sidewalls were assigned Neumann conditions. The resulting displacement at the cortex surface was 0.09 mm (data now shown). In Figure 6.3 (top panel) we show the resulting tracer concentration. We compare tracer concentrations after 15 minutes in the awake state versus the sleeping state, from 0 to 300 μm into the cortex (left), and show the time evolution of tracer concentration at a slice 100 μm below the surface (right). The applied forces in the awake state significantly slow down transport into mouse cortex. Other parameters were set as follows (see also [10, 53]):

$$\begin{aligned} &E = 800\,\mathrm{Pa},\ \nu = 0.495,\ c_0 = 2\times 10^{-8}\,\mathrm{Pa}^{-1},\ \kappa = 10^{-8}\,\mathrm{mm}^2,\ \alpha = 1,\ \ell = 0,\\ &\eta = 2\times 10^{-5},\\ &\rho_s = 10^{-3}\,\mathrm{g/mm}^3,\ \mu_f = 0.7\times 10^{-3}\,\mathrm{Pa/s},\ \beta = 0.35,\ D_0 = 5.3\times 10^{-2}\mathrm{mm}^3/\mathrm{s}. \end{aligned}$$

In the second scenario, we simulate tracer clearance from the human brain using a 3D mesh generated from the the right hemisphere of the built-in subject Bert in FreeSurfer [20]. The mesh consisted of 400000 cells, and the resulting system had 15 million degrees of freedom. Boundary conditions for this test case (in three dimensions) assume the form

$$\begin{aligned} \omega &= 0 && \text{on all boundaries},\\ p = p_0, \quad \boldsymbol{\sigma}\boldsymbol{n} &= -p_0 \arctan(t/50)\boldsymbol{n} && \text{on cortex},\\ \boldsymbol{\sigma}\boldsymbol{n} = \boldsymbol{0}, \quad \kappa\nabla p\cdot\boldsymbol{n} &= 0 && \text{on ventricles}, \end{aligned}$$

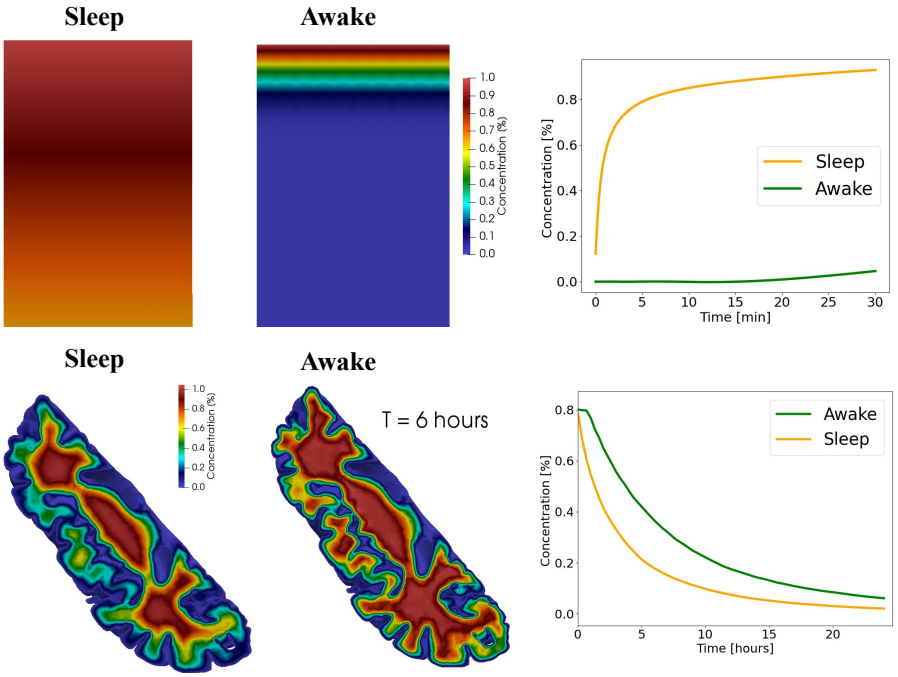

FIG. 6.3. *Example* 3. *Tracer infiltration in the mouse cortex (top panel) and tracer clearance from the human brain (bottom panel) using the stress-hindered formulation as described by* (6.4). *In the top-left we compare the sleeping versus awake state after* 15 *minutes of transport from the mouse cortex* 300 μm *into the tissue. The concentration was held fixed at the cortex. To the right, the shown time evolution* 100 μm *below the cortex indicates that transport by stress-hindered diffusion is an order of magnitude lower than for free diffusion within the cortex. In the bottom panel we show the tracer distribution in a brain slice of a human brain. In the left panel is the tracer distribution after* 12 *hours of diffusive transport. In the awake state, stress-hindered diffusion results in slightly slower clearance. In the right bottom panel, the average concentration for the entire piece of brain tissue is plotted over time.*

and the initial condition is $\omega = 1$ everywhere in the brain. Other parameters were set exactly as in the previous example, except that now $\eta = 2 \times 10^{-1}$ and the cortex pressure is $p_0 = 0.01$ mmHg. On the ventricles we imposed no-slip conditions. In Figure 6.3 (bottom panel) we show the tracer concentration in the sleeping versus awake brain after 12 hours of transport (left) and also show the time evolution of the average tracer concentration within the slice shown (right). Transport rates differ between the sleeping state versus the awake state but occur on approximately the same time scale [52] in contrast to the mouse test case. Our results from the human brain test case thus reflect differences in clearance in the awake versus sleeping state observed experimentally [15].

7. Concluding remarks. In this manuscript, we have proposed a new formulation for the transport of solutes within poroelastic structures fully saturated with an incompressible fluid, which incorporates the effect of stress-altered diffusion. Our analysis is based on a fixed-point argument combined with the generalized theory for perturbed saddle-point problems and a Banach spaces abstract result for the stress-dependent diffusion. We have shown that the discrete problem is solvable and have derived optimal error estimates under usual regularity assumptions. Additionally, we

have verified numerically that the formulation is robust with respect to variations in model parameters. The set of equations models how a tracer permeates through the brain tissue, and the incorporation of stress-altered diffusion leads to better agreement with filtration rates observed from experiments.

However, one drawback of the present formulation is its high computational cost, as it depends on several tensor and scalar secondary variables. To address this issue, we are currently investigating the analysis of simplified formulations that retain some of the appealing features of momentum conservation, parameter robustness, and amenability to analysis using perturbed saddle-point theory. Additionally, we would like to stress that our analysis does not accommodate for time dependence, which is an important matter in the context of the application that motivates the new formulation. This is one of the generalizations we are currently working on.

Other steps in the process of model refinement include the study of interfacial flow between the poroelastic structure (at the macroscale) coupled with the surrounding layer of CSF and the specific waste disposal system, which is still not well understood. For this we will also use multiple network models [32, 44], the preconditioning framework for perturbed saddle-point problems from [7], and interface couplings such as those in [11, 39, 46, 51]. Other envisaged generalizations deal with large deformations and kinematics through a more complete mixture theory following, e.g., [36, 12].

Acknowledgments. We express our gratitude for the invaluable feedback provided by four anonymous referees, whose comments have significantly enhanced the quality of the manuscript from its initial version.

REFERENCES

[1] A. Allendes, G. Campaña, F. Fuica, and E. Otarola, *Darcy's Problem Coupled with the Heat Equation Under Singular Forcing: Analysis and Discretization*, preprint, https://arxiv.org/abs/2208.12887, 2022.

[2] I. Ambartsumyan, E. Khattatov, and I. Yotov, *A coupled multipoint stress - multipoint flux mixed finite element method for the Biot system of poroelasticity*, Comput. Methods Appl. Mech. Engrg., 372 (2020), e113407.

[3] D. Arnold, F. Brezzi, and J. Douglas, *PEERS: A new mixed finite element method for plane elasticity*, Jpn. J. Appl. Math., 1 (1984), pp. 347–367.

[4] D. Arnold, R. Falk, and R. Winther, *Mixed finite element methods for linear elasticity with weakly imposed symmetry*, Math. Comp., 76 (2007), pp. 1699–1723.

[5] T. Bærland, J. J. Lee, K.-A. Mardal, and R. Winther, *Weakly imposed symmetry and robust preconditioners for Biot's consolidation model*, Comput. Methods Appl. Math., 17 (2017), pp. 377–396, https://doi.org/doi:10.1515/cmam-2017-0016.

[6] D. Boffi, F. Brezzi, and M. Fortin, *Mixed Finite Element Methods and Applications*, Springer Ser. Comput. Math. 44, Springer-Verlag, Berlin, 2013.

[7] W. Boon, M. Kuchta, K.-A. Mardal, and R. Ruiz-Baier, *Robust preconditioners and stability analysis for perturbed saddle-point problems – application to conservative discretizations of Biot's equations utilizing total pressure*, SIAM J. Sci. Comput., 43 (2021), pp. B961–B983.

[8] S. C. Brenner and L. R. Scott, *The Mathematical Theory of Finite Element Methods*, 3rd ed., Texts Appl. Math. 15, Springer-Verlag, New York, 2008, https://doi.org/10.1007/978-0-387-75934-0.

[9] F. Brezzi and M. Fortin, *Mixed and Hybrid Finite Element Methods*, Springer-Verlag, Berlin, 1991.

[10] S. Budday, R. Nay, R. de Rooij, P. Steinmann, T. Wyrobek, T. C. Ovaert, and E. Kuhl, *Mechanical properties of gray and white matter brain tissue by indentation*, J. Mech. Behav. Biomed. Mater., 46 (2015), pp. 318–330.

[11] M. Bukač, I. Yotov, R. Zakerzadeh, and P. Zunino, *Partitioning strategies for the interaction of a fluid with a poroelastic material based on a Nitsche's coupling approach*, Comput. Methods Appl. Mech. Engrg., 292 (2015), pp. 138–170.

[12] F. Costanzo and S. T. Miller, *An arbitrary Lagrangian-Eulerian finite element formulation for a poroelasticity problem stemming from mixture theory*, Comput. Methods Appl. Mech. Engrg., 323 (2017), pp. 64–97.

[13] M. Croci, V. Vinje, and M. E. Rognes, *Uncertainty quantification of parenchymal tracer distribution using random diffusion and convective velocity fields*, Fluids Barriers CNS, 16 (2019), 32.

[14] M. Croci, V. Vinje, and M. E. Rognes, *Fast uncertainty quantification of tracer distribution in the brain interstitial fluid with multilevel and quasi Monte Carlo*, Int. J. Numer. Methods Biomed. Eng., 37 (2020), e3412.

[15] P. K. Eide, V. Vinje, A. H. Pripp, K.-A. Mardal, and G. Ringstad, *Sleep deprivation impairs molecular clearance from the human brain*, Brain, 144 (2021), pp. 863–874.

[16] T. Elvsåshagen, N. Zak, L. B. Norbom, P. Ø. Pedersen, S. H. Quraishi, A. Bjørnerud, D. Alnæs, N. T. Doan, U. F. Malt, I. R. Groote, and L. T. Westlye, *Evidence for cortical structural plasticity in humans after a day of waking and sleep deprivation*, Neuroimage, 156 (2017), pp. 214–223.

[17] A. Elyes, F. Radu, and J. Nordbotten, *Adaptive poromechanics computations based on a posteriori error estimates for fully mixed formulations of Biot's consolidation model*, Comput. Methods Appl. Mech. Engrg., 347 (2019), pp. 264–294, https://doi.org/10.1016/j.cma.2018.12.016.

[18] A. Ern and J.-L. Guermond, *Theory and Practice of Finite Elements*, Appl. Math. Sci. 159, Springer-Verlag, New York, 2004, https://doi.org/10.1007/978-1-4757-4355-5.

[19] A. Ern and J.-L. Guermond, *Finite element quasi-interpolation and best approximation*, ESAIM Math. Model. Numer. Anal., 51 (2017), pp. 1367–1385, https://doi.org/10.1051/m2an/2016066.

[20] B. Fischl, *Freesurfer*, Neuroimage, 62 (2012), pp. 774–781.

[21] G. N. Gatica, *A Simple Introduction to the Mixed Finite Element Method: Theory and Applications*, Springer-Verlag, Berlin, 2014.

[22] G. N. Gatica and L. F. Gatica, *On the a priori and a posteriori error analysis of a two-fold saddle-point approach for nonlinear incompressible elasticity*, Internat. J. Numer. Methods Engrg., 68 (2006), pp. 861–892, https://doi.org/10.1002/nme.1739.

[23] G. N. Gatica, B. Gómez-Vargas, and R. Ruiz-Baier, *Analysis and mixed-primal finite element discretisations for stress-assisted diffusion problems*, Comput. Method Appl. Mech. Engrg., 337 (2018), pp. 411–438, https://doi.org/10.1016/j.cma.2018.03.043.

[24] G. N. Gatica, B. Gómez-Vargas, and R. Ruiz-Baier, *Formulation and analysis of fully-mixed finite element methods for stress-assisted diffusion problems*, Comput. Math. Appl., 77 (2019), pp. 1312–1330.

[25] G. N. Gatica, N. Heuer, and S. Meddahi, *On the numerical analysis of nonlinear twofold saddle point problems*, IMA J. Numer. Anal., 23 (2003), pp. 301–330.

[26] G. N. Gatica, C. Inzunza, and F. A. Sequeira, *A pseudostress-based mixed-primal finite element method for stress-assisted diffusion problems in Banach spaces*, J. Sci. Comput., 92 (2022), 103, https://doi.org/10.1007/s10915-022-01959-9.

[27] G. N. Gatica, A. Márquez, and W. Rudolph, *A priori and a posteriori error analyses of augmented twofold saddle point formulations for nonlinear elasticity problems*, Comput. Method Appl. Mech. Engrg., 264 (2013), pp. 23–48, https://doi.org/10.1016/j.cma.2013.05.010.

[28] D. Gilbarg and N. S. Trudinger, *Elliptic Partial Differential Equations of Second Order*, Classics Math. 224, Springer-Verlag, Berlin, 2001.

[29] V. Girault and P.-A. Raviart, *Finite Element Methods for Navier-Stokes Equations: Theory and Algorithms*, 1st ed., Springer-Verlag, Berlin, 1986.

[30] P. Grigoreva, E. N. Vilchevskaya, and W. H. Müller, *Stress and Diffusion Assisted Chemical Reaction Front Kinetics in Cylindrical Structures*, Springer-Verlag, Cham, 2019, pp. 53–72.

[31] K. E. Holter, B. Kehlet, A. Devor, T. J. Sejnowski, A. M. Dale, S. W. Omholt, O. P. Ottersen, E. A. Nagelhus, K.-A. Mardal, and K. H. Pettersen, *Interstitial solute transport in 3D reconstructed neuropil occurs by diffusion rather than bulk flow*, Proc. Natl. Acad. Sci. USA, 114 (2017), pp. 9894–9899.

[32] Q. Hong, J. Kraus, M. Lymbery, and F. Philo, *Conservative discretizations and parameter-robust preconditioners for Biot and multiple-network flux-based poroelasticity models*, Numer. Linear Algebra Appl., 26 (2019), e2242.

[33] J. J. Iliff, M. Wang, Y. Liao, B. A. Plogg, W. Peng, G. A. Gundersen, H. Benveniste, G. E. Vates, R. Deane, S. A. Goldman, E. A. Nagelhus, and M. Nedergaard, *A paravascular pathway facilitates CSF flow through the brain parenchyma and the clearance*

of interstitial solutes, including amyloid β, Sci. Transl. Med., 4 (2012), 147ra111.

[34] M. Jayadharan, E. Khattatov, and I. Yotov, *Domain decomposition and partitioning methods for mixed finite element discretizations of the Biot system of poroelasticity*, Comput. Geosci., 25 (2021), pp. 1919–1938.

[35] S. Kumar, R. Oyarzúa, R. Ruiz-Baier, and R. Sandilya, *Conservative discontinuous finite volume and mixed schemes for a new four-field formulation in poroelasticity*, ESAIM Math. Model. Numer. Anal., 54 (2020), pp. 273–299.

[36] G. E. Lang, D. Vella, S. L. Waters, and A. Goriely, *Mathematical modelling of blood-brain barrier failure and oedema*, Math. Med. Biol., 34 (2016), pp. 391–414.

[37] J. J. Lee, *Robust error analysis of coupled mixed methods for Biot's consolidation model*, J. Sci. Comput., 69 (2016), pp. 610–632.

[38] J. J. Lee, K.-A. Mardal, and R. Winther, *Parameter-robust discretization and preconditioning of Biot's consolidation model*, SIAM J. Sci. Comput., 39 (2017), pp. A1–A24.

[39] T. Li and I. Yotov, *A mixed elasticity formulation for fluid-poroelastic structure interaction*, ESAIM Math. Model. Numer. Anal., 56 (2022), pp. 1–40.

[40] A. Logg, K.-A. Mardal, and G. Wells, *Automated Solution of Differential Equations by the Finite Element Method*, Springer-Verlag, Berlin, 2012, https://doi.org/10.1007/978-3-642-23099-8

[41] X. Ma and M. D. Zoback, *Laboratory experiments simulating poroelastic stress changes associated with depletion and injection in low-porosity sedimentary rocks*, J. Geophys. Res. Solid Earth, 122 (2017), pp. 2478–2503.

[42] R. Oyarzúa and R. Ruiz-Baier, *Locking-free finite element methods for poroelasticity*, SIAM J. Numer. Anal., 54 (2016), pp. 2951–2973.

[43] W. M. Pardridge, *CSF, blood-brain barrier, and brain drug delivery*, Expert Opin. Drug Del., 13 (2016), pp. 963–975.

[44] E. Piersanti, J. J. Lee, T. Thompson, K.-A. Mardal, and M. E. Rognes, *Parameter robust preconditioning by congruence for multiple-network poroelasticity*, SIAM J. Sci. Comput., 43 (2021), pp. B984–B1007.

[45] A. Propp, A. Gizzi, F. Levrero-Florencio, and R. Ruiz-Baier, *An orthotropic electro-viscoelastic model for the heart with stress-assisted diffusion*, Biomech. Model. Mechanobiol., 19 (2020), pp. 633–659.

[46] R. Ruiz-Baier, M. Taffetani, H. D. Westermeyer, and I. Yotov, *The Biot–Stokes coupling using total pressure: Formulation, analysis and application to interfacial flow in the eye*, Comput. Method Appl. Mech. Engrg., 389 (2022), pp. 114384.

[47] F.-J. Sayas, T. S. Brown, and M. E. Hassell, *Variational Techniques for Elliptic Partial Differential Equations: Theoretical Tools and Advanced Applications*, CRC Press, Boca Raton, FL, 2019, https://doi.org/10.1201/9780429507069.

[48] Z. Shen, *Bounds of Riesz transforms on L^p spaces for second order elliptic operators*, Ann. Inst. Fourier (Grenoble), 55 (2005), pp. 173–197.

[49] R. E. Showalter, *Poroelastic filtration coupled to Stokes flow*, in *Control Theory of Partial Differential Equations*, O. Imanuvilov, G. Leugering, R. Triggiani, and B.-Y. Zhang, eds., Lect. Notes Pure Appl. Math. 242, Chapman & Hall, Boca Raton, 2005, pp. 229–241.

[50] E. Syková and C. Nicholson, *Diffusion in brain extracellular space*, Physiol. Rev., 88 (2008), pp. 1277–1340.

[51] M. Taffetani, R. Ruiz-Baier, and S. L. Waters, *Coupling stokes flow with inhomogeneous poroelasticity*, Quart. J. Mech. Appl. Math., 74 (2021), pp. 411–439.

[52] L. M. Valnes, S. K. Mitusch, G. Ringstad, P. K. Eide, S. W. Funke, and K.-A. Mardal, *Apparent diffusion coefficient estimates based on 24 hours tracer movement support glymphatic transport in human cerebral cortex*, Sci. Rep., 10 (2020), 9176.

[53] V. Vinje, A. Eklund, K.-A. Mardal, M. E. Rognes, and K.-H. Støverud, *Intracranial pressure elevation alters CSF clearance pathways*, Fluids Barriers CNS, 17 (2020), 29.

[54] L. Xie, H. Kang, Q. Xu, M. J. Chen, Y. Liao, M. Thiyagarajan, J. O'Donnell, D. J. Christensen, C. Nicholson, J. J. Iliff, T. Takano, R. Deane, and M. Nedergaard, *Sleep drives metabolite clearance from the adult brain*, Science, 342 (2013), pp. 373–377.

[55] S.-Y. Yi, *Convergence analysis of a new mixed finite element method for Biot's consolidation model*, Numer. Methods Partial Differential Equations, 30 (2014), pp. 1189–1210.

[56] S.-Y. Yi, *A study of two modes of locking in poroelasticity*, SIAM J. Numer. Anal., 55 (2017), pp. 1915–1936, https://doi.org/10.1137/16M1056109.
[57] E. Zeidler, *Nonlinear Functional Analysis and its Applications*. I, Springer-Verlag, New York, 1986.
[58] T. Zohdi and P. Wriggers, *On the effects of microstress on macroscopic diffusion processes*, Acta Mech., 136 (1999), pp. 91–107.